

**3D printers their clinical, experimental, and teaching uses.**

by

Adrien-Maxence Hespel

A thesis submitted to the Graduate Faculty of  
Auburn University  
in partial fulfillment of the  
requirements for the  
Degree of Master of Science

Auburn, Alabama  
August 1, 2015

Keywords: 3D printer, 3D rendering, teaching,  
local anesthesia, veterinary

Approved by

Judith Hudson, Chair, Professor Emeritus of Clinical Sciences  
Robert. C Cole, Clinical Lecturer of Clinical Sciences  
Dewey Wilhite, Anatomy Laboratory Coordinator

## **Abstract**

Recent technological advances in 3D printing have resulted in increased use of this technology in human medicine, and decreasing cost is making it more affordable for veterinary use. Rapid prototyping is at its early stage in veterinary medicine but clinical, educational and experimental possibilities exist. Techniques, and applications, both current and future, are explored and illustrated in this article. An experimental project evaluating the potential use of canine and feline models for the teaching of local anesthesia was also performed. These models were statistically proven to be accurate and useful for teaching purposes. The survey conducted also emphasized a desire to see more 3D models used in teaching institutions.

## **Acknowledgments**

I would like to thank Dr. Judith Hudson, Dr. Robert Cole, and Dr. Ray Wilhite for providing guidance throughout the duration of this project. Without their expertise, guidance and trust, this research project would not have been possible. The radiology team for bearing with me for all my three years of residency. Also, thank you to Dr. Jim Wright for his statistical contributions to this dissertation. Dr. Matz and Darcie Palmer with their help in the experiment. Most importantly, I would like to thank my parents and my family for all their help throughout my life. Marie de Swarte for bearing with me through up and downs. And finally all my friends who have been with me since the beginning.

## Table of Contents

Abstract.....	ii
Acknowledgments.....	iii
List of Figures.....	vi
List of Tables.....	viii
List of Terms.....	x
Introduction.....	1
Overview of the history, concepts, techniques and applications of 3D printing.....	2
<i>Technical concept</i> .....	2
<i>Applications</i> .....	10
Evaluation of a teaching model to learn local nerve blocks.....	20
<i>Experimental methods and design</i> .....	20
<i>Results</i> .....	21
<i>Discussion</i> .....	22
Transfer of knowledge concerning the 3D printer use, its maintenance, and the use of various 3D rendering softwares.....	24
<i>The 3D printer</i> .....	24
<i>The 3D software</i> .....	28

References.....	31
Appendix 1: Figures .....	36
Appendix 2: Tables .....	55

## List of Figures

<b>Figure 1 (a, b and c):</b> Evolution of the volumetric data.....	37
<b>Figure 2 (a, b and c):</b> Dorsoventral view (a) of a model of a cervical spine centered at the level of the atlanto-axial luxation.....	38
<b>Figure 3 (a and b):</b> Dorsoventral (a) and oblique (b) view of a model of an open cranium, in which a brain tumor has been reconstructed.....	39
<b>Figure 4 (a, b and c): a, b and c:</b> (a) Ventrodorsal, (b) lateral view of a prototype based on healthy cat (from the skull to the level of C7), and (c): full skeleton of a non-affected cat, which will be used as a comparison with cats affected with GM2 Gangliosidosis.....	41
<b>Figure 5 (a and b):</b> Dorso-palmar (a) and lateral (b) views of a model of the distal extremity of a horse's feet.....	43
<b>Figure 6(a, b and c):</b> Dorsoventral (a) and lateral (b) views of a prototype of the bronchial tree of a Savannah Monitor lizard, ( <i>Varanus exhantematicus</i> sp). (c) Dorsoventral view of a prototype of the bronchial tree of a Nile crocodile ( <i>Crocodylus niloticus</i> sp).....	45
<b>Figure 7:</b> Lateral view of a model of the front limb of an Anteater ( <i>Myrmecophaga Tridactyla</i> ). .....	46
<b>Figure 8:</b> Dorsoventral view of a model of the bronchial tree of a healthy feline patient....	47
<b>Figure 9:</b> Dorsoventral view of a model of the bronchial tree of a healthy canine patient..	48
<b>Figure 10:</b> Lateral view of a model of the front limb of a horse.....	49
<b>Figure 11:</b> Canine and feline mannequins used for the experiment. Before the osseous implantation.....	50
<b>Figure 12:</b> Canine mannequin illustrating the positioning of the osseous implant.....	51

**Figure 13:** Canine mannequin with the osseous model implanted.....52

**Figure 14:** Feline mannequin illustrating the positioning of the osseous implant.....53

**Figure 15:** Feline mannequin with the osseous model implanted.....54

## List of Tables

<b>Table 1:</b> Cost associated with the printing of various anatomical specimen using a standard FDM desktop printer, and a resolution of 200 microns.....	56
<b>Table 2:</b> Summary of the 31 responses to the quality survey.....	58
<b>Table 3:</b> Distribution of the responses to the first question.....	59
<b>Table 4:</b> Distribution of the responses to the second question.....	60
<b>Table 5:</b> Distribution of the responses to the third question .....	61
<b>Table 6:</b> Distribution of the responses to the fourth question.....	62
<b>Table 7:</b> Distribution of the responses to the fifth question.....	63
<b>Table 8:</b> Distribution of the responses to the sixth question.....	64
<b>Table 9:</b> Distribution of the responses to the seventh question.....	65
<b>Table 10:</b> Statistical parameters for the first question.....	66
<b>Table 11:</b> Distribution of the responses to the first question.....	67
<b>Table 12:</b> Q-Q plot for the responses of the first question.....	68
<b>Table 13:</b> Statistical parameters for the second question.....	69
<b>Table 14:</b> Distribution of the responses to the second question.....	70
<b>Table 15:</b> Q-Q plot for the responses of the second question.....	71
<b>Table 16:</b> Statistical parameters for the third question.....	72
<b>Table 17:</b> Distribution of the responses to the third question.....	73



<b>Table 18:</b> Q-Q plot for the responses of the third question.....	74
<b>Table 19:</b> Statistical parameters for the fourth question.....	75
<b>Table 20:</b> Distribution of the responses to the fourth question.....	76
<b>Table 21:</b> Q-Q plot for the responses of the fourth question.....	77
<b>Table 22:</b> Statistical parameters for the fifth question.....	78
<b>Table 23:</b> Distribution of the responses to the fifth question.....	79
<b>Table 24:</b> Q-Q plot for the responses of the fifth question.....	80
<b>Table 25:</b> Statistical parameters for the sixth question.....	81
<b>Table 26:</b> Distribution of the responses to the sixth question .....	82
<b>Table 27:</b> Q-Q plot for the responses of the sixth question.....	83
<b>Table 28:</b> Statistical parameters for the seventh question.....	84
<b>Table 29:</b> Distribution of the responses to the seventh question.....	85
<b>Table 30:</b> Q-Q plot for the responses of the seventh question.....	86

## **List of Terms**

### **Abbreviations and Acronyms**

**MCT:** multislice computed tomography

**MRI:** magnetic resonance imaging

**3D:** three dimensional

**SL:** Stereolithography

**SLS:** selective laser sintering

**FDM:** fused deposition modelling

**3DP:** 3D printing

**MJM:** multijet modelling

**MJP:** multijet printing

**UV:** ultraviolet

**PLA:** Polylactic Acid

**ABS:** Acrylonitrile Butadiene Styrene

**CAD:** computer aided design

**STL:** Surface Tessellation Language

## **I. Introduction**

This thesis is separated in 4 different chapters including the introduction. The second chapter is focused on the technological concepts behind 3D printing. This chapter was published in *Veterinary Radiology (Veterinary Radiology & Ultrasound 55.4 (2014): 347-358)* and reviews the various types of technologies available, their research and clinical use as well as explores the possible future of 3D printing. The third chapter describes the experiment conducted at Auburn using 3D models for the teaching of local anesthesia. The final and fourth chapter is an overview of the transfer of knowledge, which has been conducted to ensure the continuation of the use of the 3D printer. For further information the reader is referred to the PowerPoint that is available containing videos and explanations on how to use, clean and maintain the 3D printer and all the associated 3D software.

The printer has over the last three years been used extensively for research, teaching and clinical purposes. Collaboration with Scott-Ritchey Research Center on a project centered on a lysosomal storage disease, with Dr. Taylor on a project focused on laminitis, with the mechanical engineering group for the analysis of a carbon fiber wool, and with the geology department for stones analysis constitute the research part. Numerous companion and exotic patients affected by spinal, brain or orthopedic disorders also benefited from this technology. Teaching models for the radiology, orthopedic and medicine departments were also created.

**II. Technical concept. ( Published as ” Invited review : Applications for 3D printers in  
Veterinary Medicine ”)**

**Authors:**

Hespel Adrien-Maxence

Wilhite Ray

Hudson Judith

**Key words:**

3D model, 3D printer, Computed tomography, Teaching, medical education, rapid prototyping

**Running head:**

3D printing in veterinary medicine

**Funding:**

Funding was provided for this project by a 2013 technology grant from the Auburn University  
Information and Instruction Committee.

**Previous presentations:** N/A

Using cross-sectional imaging modalities such as multislice computed tomography (MCT), magnetic resonance imaging (MRI) or alternatively, 4D ultrasound, a high resolution 3D image can be created within minutes. 3D virtual representations of volumetric data have been proven to aid in surgical planning in human medicine and to provide a better learning experience for the surgeons involved<sup>1</sup>; however, the visualization of 3D models is limited because they are displayed and assimilated on flat screens. With technological advances in 3D printing, it is possible to physically prototype these 3D models, creating an accurate representation of the patient's anatomy.<sup>2</sup>

The Australian Biomodelling Project was formed by Paul D'Urso to investigate the use of biomodels for surgical planning, patient education and diagnosis in 1991. The methodology and results of a subsequent prospective study were released in 1999 in the Journal of Craniomaxillofacial Surgery.<sup>3</sup> A similar European Study was undertaken by the Phidias Network comprising 11 European countries with results being published in 2003.<sup>4</sup> Since that time, 3D models have been used for animals both clinically<sup>5-7</sup> as well as for research.<sup>8</sup>

This article will review the underlying technology of 3D printers, available printers, their costs and limitations, technical parameters to create and print the prototypes and the value of these models for clinical, experimental and teaching purposes.

Various rapid prototyping technologies have been employed to create models for use in human medicine since the 1980's<sup>9</sup> when at different locations researchers (Kodama, Herbert, and Hull began to investigate the possibility of creating 3D objects from light cured resin.<sup>10-14</sup> Hull

filed a patent for his process, which he called “stereolithography” in 1986 and cofounded 3D Systems for marketing purposes. Stereolithography (SL) was the technology used for creating 3D medical models in the early Australian and European studies. Other technologies include selective laser sintering (SLS), fused deposition modelling (FDM), 3D printing (3DP) and multijet modelling (MJM), also known as multijet printing (MJP). All these technologies are additive, relying on the creation of a volume by adding material one layer at a time following a predetermined pattern rather than a carving or sculpturing process in which material is removed from a raw block.

SL printers employ a low-powered ultraviolet (UV) laser that is traced across a vat filled with acrylate photopolymer or epoxy resin in a liquid form. The laser solidifies a layer of resin which is then lowered via an elevator platform into the vat. Once the first layer is completed and lowered, a new layer of fresh photocurable resin is added on top for use as raw material to be solidified by the UV light subsequently. The process is repeated as many times as necessary to complete the model. Then, excess unexposed polymer is drained away from the model. Supporting structures are removed and the model is hardened in a UV oven Additives can be used to vary the color of the resin to allow an area of interest to be colored.<sup>15</sup>

SLS is based on a concept similar to that of SL but instead of a UV laser, SLS has a high-power laser (e.g.: carbon dioxide laser), and the raw material is in powdered form, which is sintered or melted. This allows material to be made of plastic, metal, ceramic or glass.<sup>15</sup> SLS was the result of collaboration between a graduate student, Carl Deckart and one of his

professors, Joe Beaman at the University of Texas in 1984.<sup>16</sup> The research led to the formation of a manufacturing company, DTM Corp, which was later acquired by 3D Systems.

Printers based on fused deposition modeling (FDM) extrude a cable roll of specific raw material through an extrusion nozzle which melts the raw material and controls the flow of material to create a fine hair-like plastic structure. The raw material can be a thermoplastic such as Polylactic Acid (PLA) or Acrylonitrile Butadiene Styrene (ABS) or, alternatively, rubber-based material or metal materials. Fine lines of hot raw material are laid down consecutively in numerous thin layers which follow a predetermined path for the object. Scott Crump was the original developer of FDM technology and co-founded Stratasys, Ltd, which became a main competitor of 3D Systems.<sup>16</sup>

The majority of commercially available desktop printers are currently of the FDM type. These are affordable, fit in an office, are relatively easy to use and provide prints with excellent resolution. Additionally, models can be printed using different materials and/or color to enhance the realistic aspect of the prototypes or modify their physical properties, such as their rigidity or elasticity. Each printer is composed of 3 major components. The first is a simple mechanism that unrolls the spool of polymer and pushes the filament through a hot print head nozzle using a stepper motor. Secondly, a print head, which is mounted on an X and Y axis, is moved by two independent motors to permit printing in these planes. Finally, a build plate is supported by a long rod moving up and down providing the Z axis and support for the printed material. One popular line of these printers (Replicator, MakerBot, Brooklyn, New York, USA) has been

offered by MakerBot, which was founded in 2009 <sup>17</sup> [and which has been recently acquired by Stratasys (Stratasys 7665 Commerce Way Eden Prairie, MN 55344 United States Ltd.)<sup>18</sup>]. A unique type of FDM printer is offered by the RepRap (“replicating rapid”) Project, which is an open source hardware project.<sup>19</sup> The concept behind these printers is that they could be self-replicating, capable of printing the majority of their own plastic-based parts. The printers can be purchased as complete kits or can be printed by existing 3D printers from files available on-line (RepRapPro, <http://www.reprappro.com/>).

3DP printers are similar to SLS printers in that both technologies use a powder as the substrate; however, in 3DP, the printer head injects a binder into the powder rather than melting or sintering the powder. Ely Sachs and Mike Cima developed the technology working at the Massachusetts Institute of Technology. Z Corp purchased the technology but was later acquired by 3DSYSTEMS (3D Systems, Rock Hill, SC 29730 USA).<sup>16</sup>

MJM is similar to SL in that both use a photopolymer that is hardened by UV light, but a multijet printer uses print heads to jet the photopolymer and supporting wax onto a platform where the materials are then exposed to UV light.<sup>20,21</sup> The technology results in models which are overall similar in properties and quality when compared to SL.<sup>22</sup> Some printers with multiple heads allow different materials to be printed simultaneously in the same model (Objet Connex 3D printers, <http://www.stratasys.com/3d-printers/technology/polyjet-technology>).

Four key steps are required for the production of any 3D model.<sup>23</sup> The 3D data must be acquired, processed, numerically modeled and finally printed. Two primary techniques are used



to acquire 3D volumetric data. The first relies on the use of lasers to reproduce the shape of an object through a process of reverse 3D engineering. Either a single laser (laser triangulation) or a beam of laser (structured light triangulation) is projected on the object's surface, the light reflected is captured by a sensor and the data is interpolated using trigonometric triangulation.<sup>23</sup> Based on the light reflected and the distance from the sensor to the object, the shape of the model is recreated as a cloud of points, which is subsequently analyzed automatically. The redundant data points are removed and a single continuous mesh is created.

The second type of acquisition system uses transmissive scanning methods such as computed tomography, magnetic resonance imaging and 4D ultrasound.<sup>23</sup> Studies have been conducted in human medicine to evaluate the impact of MCT scanning parameters on the accuracy of 3D models. Optimal results were obtained in one study in 1996 using a helical acquisition and 2mm slices reconstructed with an overlap of 25-75%. This study also concluded that increased pitch from 1 to 1.5 was not significantly associated with a degradation of the 3D models but resulted in a significantly decreased exposure dose to the patient.<sup>24</sup> A more recent study in 2008<sup>25</sup> was conducted using 1mm slice thickness and obtained an overall better accuracy than other similarly conducted experiments using 1.5mm<sup>26</sup> or 2mm.<sup>27</sup> Furthermore, in this study,<sup>25</sup> 3D models of bone were more accurately represented when data were acquired using CT versus MRI. MRI based models were overall smaller than the true bone dimensions and were significantly more likely to contain artifacts, to be rougher in appearance and to have a discontinued mesh.<sup>25</sup>

In the second step, the medical information acquired by CT, MRI or other advanced medical imaging is exported as DICOM (digital imaging and communications in medicine) compliant files for use in commercial or open source 3D software packages for the rendering and creation of the 3D mesh. Some of the commercial packages that have been used for medical applications are *Mimics Innovation Suite*<sup>23</sup> (Materialise, Plymouth, MI 48170 USA), *Geomagic Studio*<sup>8</sup> (Raindrop Geomagic. Research Triangle Park, NC) and *ScanIP* (Simpleware, Ashburn VA). Open source software includes *Meshlab 1.3.1*<sup>5</sup> (<http://meshlab.sourceforge.net/>) and *InVesalius*<sup>2</sup> (Centro de Tecnologia da Informação Renato Archer (CTI), Brazil; <http://www.cti.gov.br/invesalius/>). After DICOM files are imported, the main steps consist of isolating the structures of interest based on their specific density (thresholding) and topography and removing any non-desired or non-anatomic information (segmentation) such as an endotracheal tube or dense feces in the colon. Multiple thresholds can be predefined so that only pixels with a gray value in the desired range are displayed.<sup>26</sup> A continuous mesh, free of any gap or defect in the rendered model, is essential (figure 1). The contours of structures are divided into large numbers of polygons to create a 3D mesh (ranging from 30,000 to millions depending on the size and complexity of the model).<sup>28</sup> Increasing the number of polygons provides a smoother and more detailed surface, but significantly increases data size and slows further post-processing. The final data is commonly exported in a computer aided design (CAD) compatible file such as the STL (Surface Tessellation Language) file format. Similar software is used to create STL files when scanners that employ reverse engineering are used to acquire a data point set.

Step three is an optional step and involves further processing of the STL files. If any

object, no matter how it was created, has to be modified in shape or form, programs such as *Autodesk 3DS Max* or *Autodesk Maya*<sup>29</sup> (Autodesk Inc., San Rafael, CA 94903 USA) are available. Alternatively, freeware such as *BRL-CAD* (<http://brlcad.org/>) or *Openscad*<sup>30</sup> (<http://www.openscad.org/>) are also available.

Finally the last step consists of importing the STL files into proprietary software associated with the printer or commercial [*netfabb Private* or *netfabb Professional*<sup>28</sup> (netfabb Software for 3D Printing, <http://www.netfabb.com>); *KISSlicer*<sup>31</sup> (<http://kisslicer.com/>)] or open source software compatible with multiple printers (eg, *ReplicatorG*, <http://www.replicat.org/start>). Some commercial software is available free of charge [*Autodesk 3D print utility* (<http://www.autodesk.com>) or netfabb Basic (<http://www.netfabb.com/>)]. Among other things, software like those listed here can be used to orientate and scale the object on the build plate in the most optimal orientation, thereby minimizing the amount of scaffolding material required and reducing the cost and time associated with printing.

In choosing the software for the final step, it is necessary to ensure that the software is compatible with the printer to be used. Alternatively, remote printing services are available through which the prototypes can be printed for a fee after STL files are provided. For all steps, chosen software must provide an accurate representation of the structure to be modeled. Additionally, some software may have a less than intuitive interface, which can be an important consideration depending on the level of expertise of the user. A complete descriptive protocol, using only free software, to go from acquisition of CT data to the final printing step has been

reported and could be used as a guideline.<sup>28</sup>

Our models were created using an FDM printer (Replicator 2, MakerBot, Brooklyn, New York, USA) from CT data. No specific CT parameters were required for performing the volume acquisition, the goal being to acquire isotropic voxels.<sup>1, 32</sup> Resulting DICOM formatted images were imported into a commercial software package [*Mimics Innovation Suite* (Materialise, Plymouth, MI 48170 USA)]. Resulting STL files were imported into proprietary software that was acquired with the printer, [*Makerware* (Makerbot, Brooklyn, NY USA)]. Current parameters used at our institution that have rendered excellent quality are 230 degrees celsius for the PLA filament on a non-heated plate and a layer thickness of 200 microns. Thinner layers, as low as 100 microns, are technically possible but would double the printing time, and are currently unnecessary because the spatial resolution of the computed tomographic examination ( $\pm 0.652\text{mm}$ ) continues to be the limiting factor.

### **Applications:**

In human medicine, 3D models have been used extensively for preplanning craniofacial and maxillofacial surgery,<sup>33-39</sup> pelvic surgery,<sup>40, 41</sup> spinal surgery,<sup>42</sup> neurosurgery,<sup>43</sup> cardiovascular surgery<sup>44-47</sup> and visceral surgery.<sup>48</sup> These models have improved the diagnosis and treatment of pathology significantly by allowing better and more accurate pre-surgical planning.<sup>1</sup> Models were found to reduce the actual operating time,<sup>3</sup> the potential surgical complications<sup>35</sup> and the cost associated with the use of surgical rooms.<sup>35</sup> Models composed of some materials, such as PLA, can be sterilized for use in the operating suite.<sup>49</sup> Furthermore, 3D

models are being used in medical schools to introduce surgical techniques to students before exposure to live patients.<sup>1, 50-52</sup> 3D printing is also currently used for radiotherapy planning to determine the optimal positioning of the radiation beam,<sup>53</sup> and for the creation of personally designed radiation shields<sup>54</sup> such as those required for radiotherapy of the face. Rapid prototyping allows the creation of customized facial prostheses such as mandibles<sup>33, 55</sup> or ears,<sup>56</sup> dental replacements,<sup>57</sup> orthodontic devices<sup>58</sup> or orthopedic prostheses<sup>59, 60</sup> by using biocompatible materials such as ceramics, polymers or metals.<sup>1</sup> Phantoms have been printed for use with PET, PET/CT<sup>61</sup>, CT and ultrasound. An SLS printer capable of printing in multiple colors (Spectrum Z510, 3DSystems, <http://www.zcorp.com/en/Products/3D-Printers/Spectrum-Z510/spage.aspx>) was used to create radioactive phantoms of human brain, human lung with a nodule, and rat brain using <sup>18</sup>F mixed with a powdered binder. The phantoms had radioactivity variability equal or less than 2%, which was similar or better than epoxy-based phantoms available at the time of the study. A similar printer was modified by other investigators and used a powder consisting primarily of cornstarch and cellulose mixed with iodine to create phantoms that approximated bone and soft tissue with the goal of creating CT phantoms that could model solid and metastatic tumors with soft boundaries.<sup>62</sup>

Additionally, bioprinting, the printing of live cells and tissues to be implanted without any autoimmune reaction, is currently an active field of research.<sup>63</sup> To enable study of angiogenesis, endothelial cells were printed within a hydrogel scaffold using a 3D printer that dispensed material from 8 microvalves onto a robotic stage.<sup>64</sup> In transplant research, multiple approaches are under investigation but they all are based on the printing of tissue in vitro by

addition of living cell layers extracted from the donor's organ of origin. In one study, electromechanical microvalves were placed at the end of robotic arms to dispense human fibroblasts, human keratinocytes, and rat neurons within a hydrogel scaffold. The study showed no significant difference in the viability of cells printed using the 3D printer and control cells which were plated manually.<sup>65</sup> This is, however, still a very experimental technology.

Veterinary clinical applications have been reported. Angular limb deformities of both the forelimb<sup>6,7</sup> and hindlimb<sup>5</sup> were treated using rapid prototyping technology. For a mixed breed dog with curvature of the antebrachium, CT data was submitted to a printing service (ProtoMed, Westminster, CO) for printing with an SL printer.<sup>6</sup> An FDM printer was used to create models of a Chihuahua with antebrachial deformities after DICOM data from CT was converted to an STL file using commercial software (ScanIP, Simpleware Ltd, Exeter, UK) and further modified with another software program<sup>7</sup> (CopyCAD Pro Design, Delcam PLC, Birmingham, UK). An SL printer (SL-190, 3DSystems) was used with STL files converted from CT images using *Mimics Innovation Suite* (Mimics Innovation Suite, Materialise, Plymouth, MI, 48170 USA) to create a model of the pelvic limbs of a German shepherd dog. These prototypes allowed surgeons to rehearse the various surgeries and evaluate possible complications. Overall, rapid prototyping was considered beneficial for the patient based on the clinical experience reported by the surgeons.<sup>5-7</sup> Reduced operating time resulted in decreased morbidity and mortality as well as decreased overall cost.<sup>5</sup> A mechanical engineer, Nate Calvin, created a prosthesis to replace the shattered upper beak of an injured bald eagle rescued in Alaska. The prosthesis allowed the bird to eat and preen its feathers while some regrowth of its beak occurred.<sup>66, 67</sup>

Rapid prototyping technology has also been used for research purposes. Ten prototypes of a canine tibia were made using an SL printer (SL-190, 3D Systems, Rock Hill, SC 29730 USA) and STL files created from CT using *Mimics Innovation Suite*. The STL files were further manipulated with additional software (*Geomagic Studio*, version 8.0, Raindrop Geomagic, Research Triangle Park, NC; SolidWorks, SolidWorks Corp, Concord, MA, USA). The prototypes were used to compare use of a custom surgical jig with a plate made of titanium for tibial plateau leveling osteotomy.<sup>8, 68, 69</sup> Models of 10 ovine stifles were created using a SLS printer<sup>25</sup> (Sinterstation HIQ Series, 3D Systems, Valencia, CA). Half of the models were based on MRI data and half were based on CT data in order to compare models based on the two methods. Resulting DICOM images were converted to STL files using Mimics software and further manipulated with 3-Matic.

At Auburn University College of Veterinary Medicine (AUCVM) , we are producing 3D models using an FDM printer (Replicator 2, Makerbot, Brooklyn, New York) after converting and editing the CT data into STL files with *Mimics Innovation Suite software* (Mimics Innovation Suite, Materialise, Plymouth, MI, 48170 USA) and importing them into *Makerware* (Makerware, Makerbot, Brooklyn, New York). 3D models were used by neurosurgeons to help them prepare for surgical treatment of atlanto-axial subluxation in a 2-pound Yorkshire-Terrier and a 4 pound miniature Chin, where placement and contouring of the surgical plates was an intricate process. For each dog, the surgeons created a preoperative template of the surgical plates, which were bent in order to clearly visualize the extent of penetration of the surgical screws inside the vertebral canal. The process provided insight into how much room would

remain for the spinal cord parenchyma (figure 2). In another case, a model allowed better assessment of a complex comminuted fracture of the axis. After evaluation of the prototype, the surgeon concluded that the fracture was sufficiently stable and surgery was unnecessary. An equine surgery has also benefited from rapid prototyping. After a horse suffered multiple severely comminuted fracture of the orbit, retro-orbital wall and temporomandibular joint, pre-operative and post-operative CT images were obtained and used for printing of models. The first model facilitated the surgical planning and reduced guesswork as has been previously reported in other cases.<sup>6</sup> The second model allowed comparison and evaluation of the results of the first surgery to determine if a second procedure was needed. Although we have printed a complex comminuted fractured pelvis to evaluate the use of our printer, we have not used the technique in a similar clinical case.

A protocol has been designed to allow use of both CT and MRI data in the same model. Prototyping of the skull can be done using computed tomographic data while MRI data can be used to include a brain lesion within the model, potentially aiding surgeons prior to biopsy or surgical resection of the lesion. This approach should help neurosurgeons to delineate boundaries for a craniotomy more precisely (figure 3) and should improve their confidence in the accurate localization of abnormal brain tissue.

Research projects at AUCVM have benefited from the use of 3D models. Rapid prototypes have been created for research on genetic disease in cats (GM2 Gangliosidosis) (figure 4) and research focused on the equine podotrochlear apparatus (figure 5). In collaboration



with the University of Utah, the bronchial tree of a Savannah Monitor lizard (*Varanus exanthematicus*)<sup>70</sup> and of a Nile Crocodile (*Crocodylus niloticus*)<sup>71</sup> were printed to illustrate airflow pathways (figures 6a, b and 6c).

A recent study in veterinary education demonstrated the value of 3D models to enhance the learning experience of undergraduate students.<sup>72</sup> This study compared the efficacy of textbooks, computerized models and 3d printed models in teaching identification of anatomical structures in MRI images of the distal equine extremity. The 3D models were printed with an Objet 3D printer by a commercial printing establishment (Industrial Plastic Fabrications, Nazeing, UK) after digital reconstructions of the equine foot were created from MRI images of the equine foot using Mimics software. Students using 3D models performed better and had a better learning experience than those using digital models or textbooks suggesting that 3D models enhance understanding of anatomical structures and their relationships.<sup>72</sup>

In comparison to the classic dissection approach which is labor intensive, rapid prototyping allows decreased cost per specimen and greater efficiency that augments the use of biological specimens to teach anatomy. To allow a hands-on approach, copies of rare anatomic specimens can be created while preserving the original and models of living patients can be created with only relatively minimal exposure to ionizing radiation (figure 7). Use of 3D models for teaching applies to all years of the veterinary curriculum. Models of the bronchial tree of a healthy feline (figure 8) and canine patient (figure 9) were created for use as a quick reference guide in the endoscopy room helping the clinician and facilitating teaching of students who are

watching the procedure.

The use of 3D models has helped human surgeons communicate with their patients.<sup>1</sup> We anticipate that prototypes will lead to improved communication with veterinary clients. By allowing owners to see and physically manipulate the 3D models of their pets, we expect that owners will comprehend better the surgical complexity, possible complications and associated cost of the procedures required to treat their pet.

There are many factors that need to be considered when choosing a printer. The type of model to be printed governs many of these factors. One limitation of our current device (Replicator2, Makerbot, Brooklyn, New York) is the maximum printable volume. The largest object that we can print is 11” in length, 6” wide, and 6.1” tall, which allows us to print the skull of a 25 kg dolichocephalic dog. To handle larger models, the object could be scaled down to reach a printable volume while keeping the original proportion or the model could be printed in multiple parts to be later assembled (Figure 10). Alternatively, a larger industrial machine could be used which could print parts up to 36” in length, 24” wide and 36” tall such as a Fortus 900mc(Stratasys Eden Prairie, MN 55344 United States).

Another factor to consider is the time required to print parts. The printing time for a skull from a dolichocephalic 25 kg dog using our current equipment averages around 6-7 hours. Faster machines are available but would still require 2-3 hours to complete a similar build. However, faster and larger machines usually come with a higher cost, a larger foot print and the need for a trained operator, therefore reducing their chances to be used easily in a clinical setting. For

example, a Stratasys Fortus 900mc measures about 2.7x1.6x2m weighs about 7,000lbs and costs around \$400,000 (Stratasys, Eden Prairie, MN 55344 United States). Files can be uploaded to commercial printing services such as Shapeways (<http://www.shapeways.com>), ProtoMed (<http://www.protomed.net/Index.htm>), Solid Concepts (<http://www.solidconcepts.com/technologies/stereolithography-sla/>) or Industrial Plastic Fabrications (<http://ipfl.co.uk/>) but the length of time from order submission to receipt of the product is an important variable limiting their usefulness in a clinical setting .

Whereas the majority of desktop FDM printers can accurately create layers of 100 microns, professional FDM (eg: Stratasys, Objet500 Connex3), SLS (eg: Stratasys Objet30 pro) and SL (eg: ProJet HD 300, 3D Systems) printers are rated at 16 micron layer thicknesses.<sup>22, 73,</sup>  
<sup>74</sup> Comparison was made between models of an anesthetized rat printed using an FDM printer (MakerBot Replicator, Brooklyn New York, USA), a printing service (Shapeways, Shapeways HQ, New York, NY 10016 USA) and a MJM printer (ProJet HD 3000, 3DSYSTEMS, Rock Hill, SC 29730 USA).<sup>28</sup> Computed tomographic data was obtained using the Albira Imaging System (Bruker, The Woodlands, TX 77381, USA) and converted into DICOM format. Meshlab v1.3.1 (<http://meshlab.sourceforge.net/>) and Netfabb Studio Basic 4.9 (<http://www.netfabb.com>) were used to optimize the image mesh, which was then exported as an STL file. This file was then printed on the MakerBot printer or the ProJet HD 3000 printer or uploaded to the Shapeways web site for commercial printing. The ProJet HD 3000 produced a model with the greatest resolution and an easily removed wax scaffold but initial cost was high and ability to print in color was limited. The cheapest option was the MakerBot but its models had the lowest

resolution, a full skeleton could not be printed, and scaffolding was more difficult to remove. Shapeways was relatively inexpensive and returned a high resolution model with variable colors but processing and filling the order required two weeks. Conversely, another study compared the accuracy and reproducibility of models printed with an FDM, an SL and a 3DP printer and found no significant difference between the different methods of printing.<sup>75</sup> Unfortunately, the actual printers used were not specified.

The overall cost associated with a 3d printer depends primarily on which type is chosen. Large industrial SL devices range between \$70,000 and \$400,000. Smaller devices such as FDM desktop printers cost between \$1500 and \$2500.<sup>76-78</sup> Cheaper open source hardware printers are available but these may require modification or technical expertise to operate.<sup>19</sup> The cost of basic plastic raw material depends on which type of rapid prototyping process is used: a kilogram of a powdered plastic to be used in a SLS printer averages about \$500, a liter of a photocurable resin ranges from \$100 to \$200, while 1 kg of spool for a FDM printer averages about \$50. However, a larger range of materials with different physical properties such as rigidity or elasticity are available for each printer and may affect their prices. These materials with modified biomechanics properties are especially useful when printing moving parts but are of little use when creating static anatomic models. Additionally, there are printers that are capable of printing multiple colors simultaneously whereas others are capable of printing only one color. The use of an FDM printer has allowed us to print 3D models for clinical cases for a very low cost (Table 1) and, depending on the size of the model, the cost of a model rarely exceeds \$5.

As with any other technology, maintenance should also be factored into the equation. Because FDM printer technology is relatively young and the specific printer used in our institution is less than 1 year-old, the life expectancy of our machine is currently unknown. However, we have disassembled our printer for cleaning and individual components are sold separately by the manufacturer suggesting that replacement of parts by the user will be relatively simple.

3D printer technology is providing veterinary medicine with a powerful tool to facilitate surgical planning, enhance the teaching of students, promote research and improve client communication. The use of rapid prototyping is expected to increase as volumetric acquisition in MRI and 4D ultrasound<sup>45</sup> become more routine. Finally, as technology evolves, more materials, including tissues, should be printable as suggested by current research on the printing of transplantable organs.<sup>58</sup> The use of 3D printers is currently reported as being common in human radiology departments and has been integrated into the clinical routine.<sup>45</sup> Radiologists have the anatomical and technical knowledge to use the devices and correct for any possible artifacts affecting the anatomy.<sup>1</sup>

### **III. Evaluation of a teaching model for local nerve blocks.**

#### **Experimental methods and design:**

In order to evaluate the efficacy of 3D printing, stuffed canine and feline models with 3D printed bones were compared to regular stuffed animal models. Trainees were provided with a set of normal bones printed to the scale of the stuffed animals, a set of stuffed models with implanted bones, and a set of non-implanted stuffed models (figures 11-15). Both canine and feline examples were available and the focus was on the regional anesthesia of the forelimb. The trainees were able to review the normal anatomy using both the non-implanted and implanted 3D models. The purpose of the training session being to learn how to perform local forelimb nerve blocks, the trainees were asked at the end of the lab to fill a quality scaled survey. This survey had a Likert scale ranging from a grade of 1 to 5 evaluating 7 different statements. The statements were as follow:

- The canine osseous model non implanted helped me to recall the normal anatomy
- The feline osseous model non implanted helped me to recall the normal anatomy
- The canine osseous model implanted allowed me to palpate the structures of interest and gave me confidence for my needle placement
- The feline osseous model implanted allowed me to palpate the structures of interest and gave me confidence for my needle placement

- The canine model was an adequate representation of a healthy dog
- The feline model was an adequate representation of a healthy cat
- I would like to see 3D models used more commonly for teaching purposes

The rating of the survey was as follows: 1 being total disagreement, 3 neutral and 5 total agreement with the statements. The 7 questions were used to subjectively evaluate the user's perception of the 3D models, as well as the trainee's likelihood to reuse 3D models for future teaching purposes. The results of the survey were plotted in an Excel (Microsoft Corporation, Redmond, WA spreadsheet). Statistical analysis was performed with using statistical software (SAS, Cary, NC 27513-2414, USA) with a Proc T-Test to evaluate any possible correlations amongst the results of the survey. Significance for all analyses was set at  $p \leq 0.05$ . All numerical data was reported as mean plus or minus standard deviation.

### **Results:**

A total of 31 trainees attended the lab and completed the survey (table 2). Of these, 11/31 (35.4%) were veterinary technicians, 16/31 (51.6%) were final year veterinary students and 4/31 (12.9%) were veterinarians. The average score and median score for the first question were 4.27 and 4 respectively (tables 3, 10 and 11), for the second question 4.27 and 4 respectively (tables 4, 13 and 14), for the third question 4.14 and 4 respectively (tables 5, 16 and 17), for the fourth question 4.15 and 4 respectively (tables 6, 19 and 20), for the fifth question 3.48 and 3 respectively (tables 7, 22 and 23), for the sixth question 3.56 and 3 respectively (tables 8, 25 and

26), and for the seventh question 4.65 and 5 respectively (tables 9, 28 and 29). When using a Proc T-Test, for all the questions, the participants were significantly more likely to choose a response superior or equal to 3 ( $p < 0.001$ ) indicating agreement to very strong agreement to statements in the questionnaire (tables 10, 13, 16, 19, 22 and 25). Q-Q plot of scores were also performed for each question (tables 12, 15, 18, 21, 24, 27 and 30) and all were consistent with a non-normal distribution of the data.

### **Discussion:**

Statistically, all participants were in agreement with the questionnaire, indicating a high level of satisfaction with both non-implanted and implanted 3D models. The questions which had the lowest overall mean score were questions 5 and 6. This can easily be explained based on the fact that the mannequins purchased for the experiments were stuffed toys and therefore far from being perfectly anatomically accurate. It is the author's opinion that these questions would have had a better overall score if the mannequins had been more anatomically accurate. The question which had the highest overall median and mean score was question 7, which strongly indicates that participants have embraced the idea of using 3D models for teaching purposes and are open to their use in a teaching environment.

However, this study also has limitations. First of all the mannequins used were not designed to be anatomically accurate and that may have impaired the educational potential of the project. In this study there was also no gold standard to compare the models with. Ideally a similar project could be carried on using both 3D printed models within mannequins in



comparison with real limbs of deceased patients. A method of tracking the position of the needle upon insertion would also be optimal, this could be done using contrast material such as methylene blue and dissecting both the cadaver limbs and the mannequins. This would allow objective evaluation on the performance of the trainees.

#### **IV. Transfer of knowledge concerning the 3D printer use, its maintenance, and the use of various 3D rendering software.**

The reader is strongly encouraged to refer to the attached PowerPoint (Microsoft Corporation, Redmond, WA spreadsheet) presentation as many of the points are explained through videos.

This section is divided in two main sections: The 3D printer itself and the associated 3D software.

##### **The 3D Printer**

The 3D printer is composed of numerous parts: The build plate provides support for the build and moves on the Z-plane. The two step-by-step motors provide motion along the X and Y axis. The endless screw allows the displacement of the build plate on the Z axis. On the left and on the front of the assembly there are two fans. The one on the left provides cool air on the model to allow quick cooling and solidification of the plastic. The one on the front keeps the extruder at an adequate temperature.

On the front of the printer, an LCD screen is available for all the menuing options including *build from SD card, preheat, utilities, monitor mode, change filament, level the build plate, home axes, jog mode, run Startup Script and info and settings.*

Within the Powerpoint presentations videos explaining the routine procedures are available; however, this is a brief “how to” on the most common procedures: **Load filament:** The filament can be loaded once the printing head is at an appropriate temperature. Make sure that the filament terminates sharply (cut it if needed); then, put the filament in the hole of the printing

head from the top while depressing the spring on the right side. Apply mild pressure downwards. Once the filament is engaged in the step-by-step motor, you will feel mild traction of the filament from your fingers and melted plastic will appear at the level of the nozzle.

**Unload filament:** To unload the filament, wait until the printing head is at an appropriate temperature. Start by loading the filament to ensure better unloading. Once a small amount of plastic has been passed through, select unloading. Grab the filament between your fingers and pull gently on it. The filament will come without any need to press on the spring. Once the filament is removed, make sure that there is no plastic remaining within the step-by-step motor. If necessary, cleaning may be useful.

To maintain proper and reliable use of the printer adequate and routine maintenance must be performed. These maintenance procedures include: cleaning, greasing, changing the build plate and leveling the build plate.

**Cleaning:** Cleaning the step-by-step motor should be done regularly as part of routine maintenance procedures. However, cleaning the motor is mandatory after a filament jam. If the filament were to get stuck and the motor continued to run, the filament would be eroded and a large amount of plastic dust would accumulate at this level. Ideally, you should unload the filament, keep the motor spinning and blow a bit of compressed air on the gears. If a large amount of material is stuck, a small tooth brush will easily remove the residue.

**Greasing:** Ideally, the cleaning and greasing procedure should be performed about every 90-100 hours. First the 3 axes need to be cleaned using a dry cloth. Once these are cleaned, a small

amount of synthetic PTFE grease should be reapplied on all axes. A small paint brush can be used to facilitate that.

**Changing the build plate:** Remove the previous masking tape and use a small amount of alcohol to clean every trace of remaining glue. Once the plate is cleaned, reapply the new masking tape and fold the edges to provide appropriate coverage. Make sure that no air gets trapped underneath it.

**Leveling the build plate:** Levelling the build plate can be a very challenging procedure. There are 3 main screws under the plate and tightening them will drop the build plate while loosening them will bring the plate closer to the printer head. The plate must be about 100 microns from the printer head (equivalent to the thickness of a thin business card). The level can be adjusted using the business card provided, the micrometer, the levelling plate object or usually a combination of the three.

**Dismantling the printer for repair:** Unfortunately, like all machines, the 3D printer also has failures, and the operator should know how to fix them. First, you need to dismantle the machine. To do so, after unloading the filament, remove the two bottom long bolts holding the assembly together. The bolts, two plastic spacers, the fan protector and the fan will come loose. Disconnect the electric supply to the fan if needed. The step-by-step motor will just pop-out from the back. Disconnect its power supply from the top if needed. This should provide all access required for cleaning/maintenance procedures. The fan, placed laterally, is held in place by two long screws. If necessary, you can also remove the fan. Adjacent to this fan, on the side where the printing assembly is, there are two little bolts holding the plastic down to the heat sink. These screws

become loose and need to be tightened regularly. The machine reassembly is fairly straight forward. Make sure all the screws are tightened properly.

**Filament jam:** From time to time the PLA filament can jam within the printing nozzle. If there is a bad or very bad filament jam, some plastic material may get trapped at the level of the nozzle or in the nozzle. In a simple case you just need to disassemble the machine, preheat the nozzle for 10 minutes to make sure the filament will be easily removed and take it out with a pair of needle nose pliers. In a complicated case, the jam will be only inside the nozzle and nothing will be protruding making its removal difficult. In that case, after warming up the printer, use the tip of a large bore needle to pry the proximal part of the plastic out. As soon as some plastic is reachable outside of the nozzle grab it with the needle pliers and remove it slowly. In very extreme cases, an 18 gauge needle can be used to “drill” out any plastic obstructing the nozzle; however, be careful not to damage the outer extremity of the nozzle head.

**Replacing the fan:** In front of the printing assembly there is a cooling fan. If the fan is damaged, replacing it is fairly straight forward. First, print new fan blades using a file found at <https://www.thingiverse.com/thing:186979/#files>. It has to be a counter-clockwise fan. Once the fan is printed, disassemble the machine until the fan assembly is freely movable and electronically disconnected. Remove the old fan. Once the old blades are removed, make sure that the surface of the spinning part is smooth. Take the new blades and press them on the spinning part. No need to glue because it's a press fit, but go slowly or the new blades may break. Once the fan blades are replaced, just reassemble the fan assembly.

### **3D Software**

The 3D software used for preparing 3D models for printing include Mimics Innovation Suite (Materialise, Plymouth, MI 48170 USA, Autodesk (Autodesk Inc., San Rafael, CA 94903 USA), ReplicatorG (<http://www.replicat.org/start>) and Makerware (Makerbot, Brooklyn, NY USA). The key software for the production and creation of 3D models is Mimics. There are numerous ways to create the 3D masks including: thresholding, dynamic region growing, Boolean operation, flood fill and multiple slice edit.

Thresholding is the quickest and easiest way to make 3D models of osseous structures. Right click in top tabs, choose “thresholding”. You can change which type of body parts to be included in your model based on their Hounsfield units. Numerous preset parameters are available such as “bone dense”. Two tick boxes are also available: “fill holes,” which makes a more homogeneously filled model and “keep largest” which would only keep the largest structure of the defined HU units. The later can be useful if you are doing body parts such as legs.

Dynamic region growing is fairly useful for doing soft tissue models, such as brain tumors, airways or contrast enhancing lesions. Just select where you want your ROI to start from and the maximum and minimum HU range that you want to include. The check boxes “fill cavities” and “multiple slices” need to be checked.

The Boolean operations allow you to “minus”, “unite” or “intersect” various masks. Let’s say that you have done all the bones of a skull and a leg as one single mask. If you have already

taken the time to separate the leg from the head rather than segmenting the head manually, you can just perform a subtraction.

Flood fill is a very useful and potent tool for working with soft tissues particularly if the margins are not well defined. The calibration tool determines the upper and lower HU tolerable limits. Left click and drag towards the area you want to select to incorporate all the pixels within the HU range.

The multiple slice edit feature can save time. If you are manually segmenting a fairly large structure of homogeneous texture and shape, you can perform your segmentation on only a few “representative” slices and ask the computer to interpolate the remainder of them.

Once the 3D mask or the 3D model have been generated you can alter it to optimize printing. To do so you can simplify it, smooth it or just simply edit it.

The smoothing parameters I have empirically used after numerous trials are: Iterations: 500.

This reflects how many times the computer will process the model. The more iterations the better the results but the more computing power you need. Smooth factor: 200. This is the thresholding level for the polygons.

Simplifying will decrease the number of polygons of a model without significantly affecting its appearance and accuracy. A lesser number of polygons means a lighter object for the computer to process and also a faster printing time. The parameters which have worked the best for me are tolerance: 0.20 mm, edge tolerance: 15.00 degrees, and iterations: 500

3D Edition: The 3D edition allows you to perform any of the operations above directly in the 3D model rather than using the axial, coronal or sagittal planes.

Numerous further advanced technical parameters and instruction are available in the PowerPoint created for the transfer of knowledge, and the user is once again strongly encouraged to consult that presentation for further information.



## VII. References

1. Rengier F, Mehndiratta A, von Tengg-Kobligh H, Zechmann CM, Unterhinninghofen R, Kauczor H-U, et al. 3D printing based on imaging data: review of medical applications. *International journal of computer assisted radiology and surgery*. 2010;**5**: 335-341.
2. Silva DN, Gerhardt de Oliveira M, Meurer E, Meurer MI, Lopes da Silva JV, Santa-Bárbara A. Dimensional error in selective laser sintering and 3D-printing of models for craniomaxillary anatomy reconstruction. *Journal of cranio-maxillofacial surgery*. 2008;**36**: 443-449.
3. D'Urso PS, Barker TM, Earwaker WJ, Bruce LJ, Atkinson RL, Lanigan MW, et al. Stereolithographic biomodelling in cranio-maxillofacial surgery: a prospective trial. *Journal of cranio-maxillofacial surgery*. 1999;**27**: 30-37.
4. Wulf J, Vitt K, Erben C, Bill J, Busch L. Medical biomodelling in surgical applications: results of a multicentric European validation of 466 cases. *Studies in health technology and informatics*. 2003;**94**: 404.
5. Harrysson OL, Cormier DR, Marcellin-Little DJ, Jajal K. Rapid prototyping for treatment of canine limb deformities. *Rapid Prototyping Journal*. 2003;**9**: 37-42.
6. Dismukes DI, Fox DB, Tomlinson JL, Essman SC. Use of radiographic measures and three-dimensional computed tomographic imaging in surgical correction of an antebrachial deformity in a dog. *Journal of the American Veterinary Medical Association*. 2008;**232**: 68-73.
7. Crosse K, Worth A. Computer-assisted surgical correction of an antebrachial deformity in a dog. *Veterinary and Comparative Orthopaedics and Traumatology*. 2010;**23**: 354.
8. Marcellin-Little DJ, Harrysson OL, Cansizoglu O. In vitro evaluation of a custom cutting jig and custom plate for canine tibial plateau leveling. *American journal of veterinary research*. 2008;**69**: 961-966.
9. Giannatsis J, Dedoussis V. Additive fabrication technologies applied to medicine and health care: a review. *The International Journal of Advanced Manufacturing Technology*. 2009;**40**: 116-127.
10. Powers D, Edgin W, Tabatchnick L. Stereolithography: a historical review and indications for use in the management of trauma. *The Journal of cranio-maxillofacial trauma*. 1998;**4**: 16.
11. Bártolo PJ. *Stereolithography: materials, processes and applications*: Springer, 2011.
12. Kodama H. Automatic method for fabricating a three-dimensional plastic model with photo-hardening polymer. *Review of Scientific Instruments*. 1981;**52**: 1770-1773.
13. Herbert AJ. Solid object generation. *J Appl Photo Eng*. 1982;**8**: 185-188.
14. Hull CW. Method for production of three-dimensional objects by stereolithography. Google Patents, 1990.
15. McGurk M, Amis A, Potamianos P, Goodger N. Rapid prototyping techniques for anatomical modelling in medicine. *Annals of the Royal College of Surgeons of England*. 1997;**79**: 169.

16. Austin DoMETUoTa. Selective Laser Sintering, Birth of an Industry. 2013 May 30th, 2013 [cited 1.19.14]; Available from: [http://www.me.utexas.edu/news/2012/0712\\_sls\\_history.php](http://www.me.utexas.edu/news/2012/0712_sls_history.php)
17. Makerbot. Makerbot FAQ. 2012 [cited 1.19.2014]; Available from: <http://www.makerbot.com/faq/>
18. Sharma R. The real reason Stratasys bought MakerBot. Forbes 2013 [cited 1.19.2014]; Available from: <http://www.forbes.com/sites/rakeshsharma/2013/09/24/stratasys-bold-moves-a-conversation-with-company-chairman-scott-crump/>
19. Kentzer J, Koch B, Thiim M, Jones RW, Villumsen E. An open source hardware-based mechatronics project: The replicating rapid 3-D printer. *Mechatronics (ICOM), 2011 4th International Conference On: IEEE*, 2011;1-8.
20. 3DSYSTEMS. 3D Systems Multijet Printing Process. 2014 [cited 1.21.2014]; Available from: <http://www.3dsystems.com/3d-media/3d-printing-process-mjm>
21. 3DSYSTEMS. MultiJet Printing 2014 [cited 2014 1.29.14]; Available from: <http://www.3dsystems.com/quickparts/prototyping-pre-production/multijet-printing-mjp>
22. 3DSYSTEMS. 3D Process Comparison. 2014 [cited 1.21.2014]; Available from: <http://www.3dsystems.com/quickparts/prototyping-pre-production/process-comparison>
23. Hieu L, Zlatov N, Vander Sloten J, Bohez E, Khanh L, Binh P, et al. Medical rapid prototyping applications and methods. *Assembly Automation*. 2005;**25**: 284-292.
24. Hopper KD, Pierantozzi D, Potok PS, Kasales CJ, TenHave TR, Meilstrup JW, et al. The quality of 3D reconstructions from 1.0 and 1.5 pitch helical and conventional CT. *Journal of computer assisted tomography*. 1996;**20**: 841-847.
25. White D, Chelule K, Seedhom B. Accuracy of MRI vs CT imaging with particular reference to patient specific templates for total knee replacement surgery. *The International Journal of Medical Robotics and Computer Assisted Surgery*. 2008;**4**: 224-231.
26. Barker T, Earwaker W, Lisle D. Accuracy of stereolithographic models of human anatomy. *Australasian Radiology*. 1994;**38**: 106-111.
27. Lill W, Solar P, Ulm C, Watzek G, Blahout R, Matejka M. Reproducibility of three-dimensional CT-assisted model production in the maxillofacial area. *British Journal of Oral and Maxillofacial Surgery*. 1992;**30**: 233-236.
28. Doney E, Krumdick L, Diener J, Wathen C, Chapman S, Stamile B, et al. 3D Printing of Preclinical X-ray Computed Tomographic Data Sets. *Journal of visualized experiments: JoVE*. 2012.
29. Griffey J. Chapter 4: Absolutely Fab-ulous. *Library Technology Reports*. 2012;**48**: 21-24.
30. Gonzalez-Gomez J, Valero-Gomez A, Prieto-Moreno A, Abderrahim M. A new open source 3d-printable mobile robotic platform for education. *Advances in autonomous mini robots*: Springer, 2012;49-62.
31. Frauenfelder M. *Make: Ultimate Guide to 3D Printing 2014*: Maker Media, Inc., 2013.
32. Mahesh M. The AAPM/RSNA Physics Tutorial for Residents Search for Isotropic Resolution in CT from Conventional through Multiple-Row Detector1. *Radiographics*. 2002;**22**: 949-962.

33. D'Urso PS, Effeney DJ, Earwaker WJ, Barker TM, Redmond MJ, Thompson RG, et al. Custom cranioplasty using stereolithography and acrylic. *British Journal of Plastic Surgery*. 2000;**53**: 200-204.
34. Faber J, Berto PM, Quaresma M. Rapid prototyping as a tool for diagnosis and treatment planning for maxillary canine impaction. *American journal of orthodontics and dentofacial orthopedics*. 2006;**129**: 583-589.
35. Mavili ME, Canter HI, Saglam-Aydinatay B, Kamaci S, Kocadereli I. Use of three-dimensional medical modeling methods for precise planning of orthognathic surgery. *Journal of Craniofacial Surgery*. 2007;**18**: 740-747.
36. Müller A, Krishnan KG, Uhl E, Mast G. The application of rapid prototyping techniques in cranial reconstruction and preoperative planning in neurosurgery. *Journal of Craniofacial Surgery*. 2003;**14**: 899-914.
37. Olszewski R. Surgical Engineering in Cranio-Maxillofacial Surgery: A Literature Review. *Journal of Healthcare Engineering*. 2012;**3**: 53-86.
38. Poukens J, Haex J, Riediger D. The use of rapid prototyping in the preoperative planning of distraction osteogenesis of the cranio-maxillofacial skeleton. *Computer Aided Surgery*. 2003;**8**: 146-154.
39. Kermer C, Lindner A, Friede I, Wagner A, Millesi W. Preoperative stereolithographic model planning for primary reconstruction in craniomaxillofacial trauma surgery. *Journal of cranio-maxillofacial surgery*. 1998;**26**: 136-139.
40. Guarino J, Tennyson S, McCain G, Bond L, Shea K, King H. Rapid prototyping technology for surgeries of the pediatric spine and pelvis: benefits analysis. *Journal of Pediatric Orthopaedics*. 2007;**27**: 955-960.
41. Hurson C, Tansey A, O'Donnchadha B, Nicholson P, Rice J, McElwain J. Rapid prototyping in the assessment, classification and preoperative planning of acetabular fractures. *Injury*. 2007;**38**: 1158-1162.
42. Paiva WS, Amorim R, Bezerra DAF, Masini M. Application of the stereolithography technique in complex spine surgery. *Arquivos de neuro-psiquiatria*. 2007;**65**: 443-445.
43. Giesel FL, Hart AR, Hahn HK, Wignall E, Rengier F, Talanow R, et al. 3D reconstructions of the cerebral ventricles and volume quantification in children with brain malformations. *Academic radiology*. 2009;**16**: 610-617.
44. Kim MS, Hansgen AR, Wink O, Quaipe RA, Carroll JD. Rapid Prototyping A New Tool in Understanding and Treating Structural Heart Disease. *Circulation*. 2008;**117**: 2388-2394.
45. Armillotta A, Bonhoeffer P, Dubini G, Ferragina S, Migliavacca F, Sala G, et al. Use of rapid prototyping models in the planning of percutaneous pulmonary valved stent implantation. *Proceedings of the Institution of Mechanical Engineers, Part H: Journal of Engineering in Medicine*. 2007;**221**: 407-416.
46. Wurm G, Tomancok B, Pogady P, Holl K, Trenkler J. Cerebrovascular stereolithographic biomodeling for aneurysm surgery: technical note. *Journal of neurosurgery*. 2004;**100**: 139-145.
47. von Tengg-Kobligh H, Weber T, Rengier F, Kotelis D, Geisbüsch P, Böckler D, et al. Imaging modalities for the thoracic aorta. *Journal of cardiovascular surgery*. 2008;**49**: 429-447.

48. Hiramatsu H, Yamaguchi H, Nimi S, Ono H. Rapid prototyping of the larynx for laryngeal frame work surgery]. *Nihon Jibiinkoka Gakkai kaiho*. 2004;**107**: 949.
49. Berman P S. Advent of 3D printing based on MDCT data. *Eur Radiol*. 2009; **19**: S397.
50. Bruyère F, Leroux C, Brunereau L, Lermusiaux P. Rapid prototyping model for percutaneous nephrolithotomy training. *Journal of Endourology*. 2008;**22**: 91-96.
51. Kalejs M, von Segesser LK. Rapid prototyping of compliant human aortic roots for assessment of valved stents. *Interactive cardiovascular and thoracic surgery*. 2009;**8**: 182-186.
52. Waran V, Narayanan V, Karuppiah R, Pancharatnam D, Chandran H, Raman R, et al. Injecting Realism in Surgical Training—Initial Simulation Experience With Custom 3D Models. *Journal of Surgical Education*. 2013.
53. Sun S-P, Wu C-J. The application of full scale 3D anthropometric digital model system in radiotherapy positioning and verification. *Biomedical Engineering: Applications, Basis and Communications*. 2004;**16**: 173-179.
54. Zemnack C, Woodhouse SA, Gewanter RM, Raphael M, Piro JD. Rapid prototyping technique for creating a radiation shield. *The Journal of Prosthetic Dentistry*. 2007;**97**: 236-241.
55. Singare S, Liu Y, Li D, Lu B, Wang J, He S. Individually prefabricated prosthesis for maxilla reconstruction. *Journal of Prosthodontics*. 2007.
56. Ciocca L, Mingucci R, Gassino G, Scotti R. CAD/CAM ear model and virtual construction of the mold. *The Journal of Prosthetic Dentistry*. 2007;**98**: 339-343.
57. Lee M-Y, Chang C-C, Ku Y. New layer-based imaging and rapid prototyping techniques for computer-aided design and manufacture of custom dental restoration. *Journal of Medical Engineering & Technology*. 2008;**32**: 83-90.
58. 3DSYSTEMS. Orthodontics. 2014 [cited 02.09.2014]; Available from: <http://www.toptobottomdental.com/orthodontics.html>
59. Dai K-R, Yan M-N, Zhu Z-A, Sun Y-H. Computer-aided custom-made hemipelvic prosthesis used in extensive pelvic lesions. *The Journal of arthroplasty*. 2007;**22**: 981-986.
60. Harrysson OL, Hosni YA, Nayfeh JF. Custom-designed orthopedic implants evaluated using finite element analysis of patient-specific computed tomography data: femoral-component case study. *BMC Musculoskeletal Disorders*. 2007;**8**: 91.
61. Miller MA, Hutchins GD. Development of anatomically realistic PET and PET/CT phantoms with rapid prototyping technology. *Nuclear Science Symposium Conference Record, 2007 NSS'07 IEEE*: IEEE, 2007;4252-4257.
62. Yoo TS, Hamilton T, Hurt DE, Caban J, Liao D, Chen DT. Toward quantitative X-ray CT phantoms of metastatic tumors using rapid prototyping technology. *Biomedical Imaging: From Nano to Macro, 2011 IEEE International Symposium on*: IEEE, 2011;1770-1773.
63. Mironov V, Boland T, Trusk T, Forgacs G, Markwald RR. Organ printing: computer-aided jet-based 3D tissue engineering. *TRENDS in Biotechnology*. 2003;**21**: 157-161.
64. Lee V, Lee W, Yoo S, Dai G. Construction of vasculature structure within fluidic channel using three-dimensional bio-printer. *Bioengineering Conference (NEBEC), 2011 IEEE 37th Annual Northeast*: IEEE, 2011;1-2.

65. Lee W, Lee V, Polio S, Fischer K, Lee J-H, Park J-K, et al. Three-dimensional cell-hydrogel printer using electromechanical microvalve for tissue engineering. *Solid-State Sensors, Actuators and Microsystems Conference, 2009 TRANSDUCERS 2009 International*: IEEE, 2009;2230-2233.
66. Group KE. Prosthetic Eagle Beak. 2007 [cited 2014 2.10.2014]; Available from: <http://www.kineticengineeringgroup.com/portfolio-misc-eagle.html>
67. The Guardian G. Restoring Beauty. September 8, 2012 [cited 2014 2.10.2014]; Available from: <http://www.theguardian.com/science/grrlscientist/2012/sep/08/1>
68. Harrysson OL, Cansizoglu O, Marcellin-Little DJ, Cormier DR, West II HA. Direct metal fabrication of titanium implants with tailored materials and mechanical properties using electron beam melting technology. *Materials Science and Engineering: C*. 2008;**28**: 366-373.
69. Hildreth III BE, Marcellin-Little DJ, Roe SC, Harrysson OL. In vitro evaluation of five canine tibial plateau leveling methods. *American journal of veterinary research*. 2006;**67**: 693-700.
70. Schachner ER, Cieri RL, Butler JP, Farmer C. Unidirectional pulmonary airflow patterns in the savannah monitor lizard. *Nature*. 2013.
71. Schachner ER, Hutchinson JR, Farmer C. Pulmonary anatomy in the Nile crocodile and the evolution of unidirectional airflow in Archosauria. *PeerJ*. 2013;**1**: e60.
72. Preece D, Williams SB, Lam R, Weller R. "Let's Get Physical": Advantages of a physical model over 3D computer models and textbooks in learning imaging anatomy. *Anatomical sciences education*. 2013.
73. Stratasys. Objet500 Connex Printer Specifications. 2014 [cited 1.30.14]; Available from: <http://www.stratasys.com/3d-printers/design-series/precision/objet500-connex3>
74. Stratasys. Objet30 Pro Specifications. 2014 [cited 1.30.14]; Available from: <http://www.stratasys.com/3d-printers/design-series/precision/objet30-pro>
75. Fitzwater KL, Marcellin-Little DJ, Harrysson OL, Osborne JA, Poindexter EC. Evaluation of the effect of computed tomography scan protocols and freeform fabrication methods on bone biomodel accuracy. *American journal of veterinary research*. 2011;**72**: 1178-1185.
76. Makerbot. Makerbot Replicator Mini. 2014 [cited 1.30.2014]; Available from: <http://store.makerbot.com/replicator-mini>
77. Makerbot. Makerbot Replicator. 2014 [cited 1.30.2014]; Available from: <http://store.makerbot.com/replicator>
78. Cubify. Cube Store. 2014 [cited 1.30.14]; Available from: <http://cubify.com/cube/store.aspx>

## **Appendix 1: Figures**

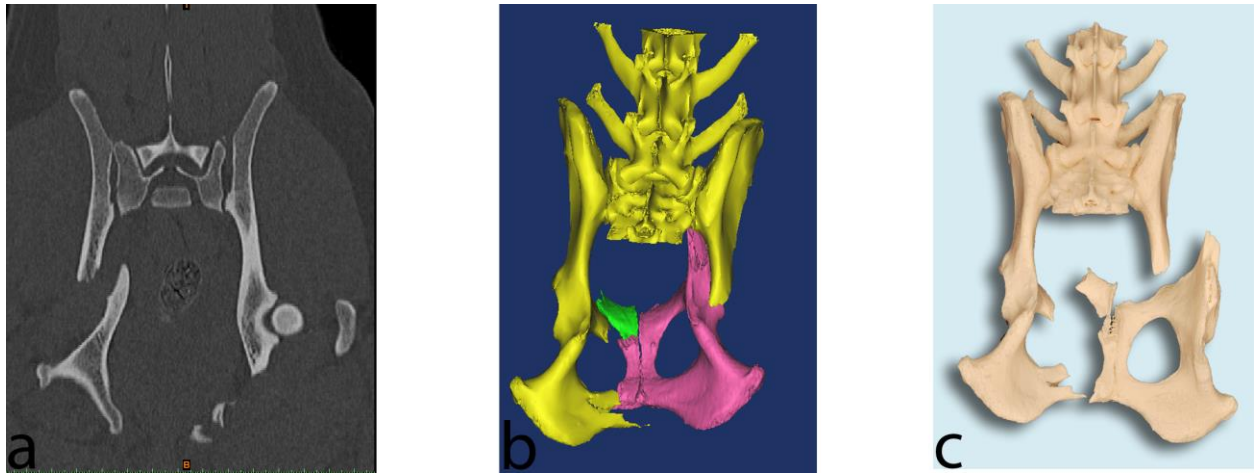
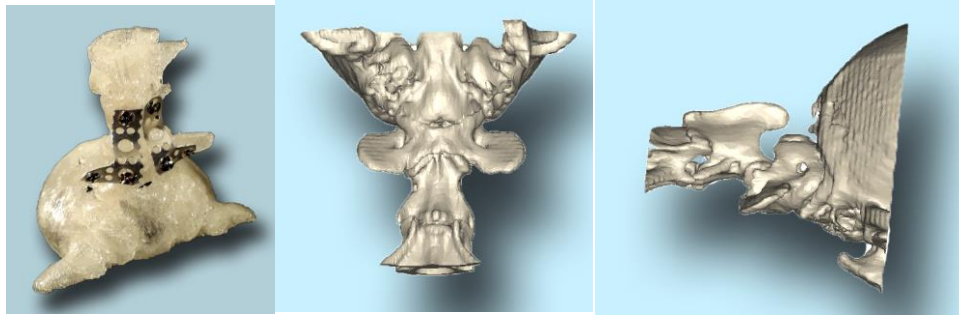


**Figure 1 (a, b and c):** Evolution of the volumetric data.

**a:** Image acquired from the CT and ready for transfer to the dedicated post-processing workstation as a DICOM file.

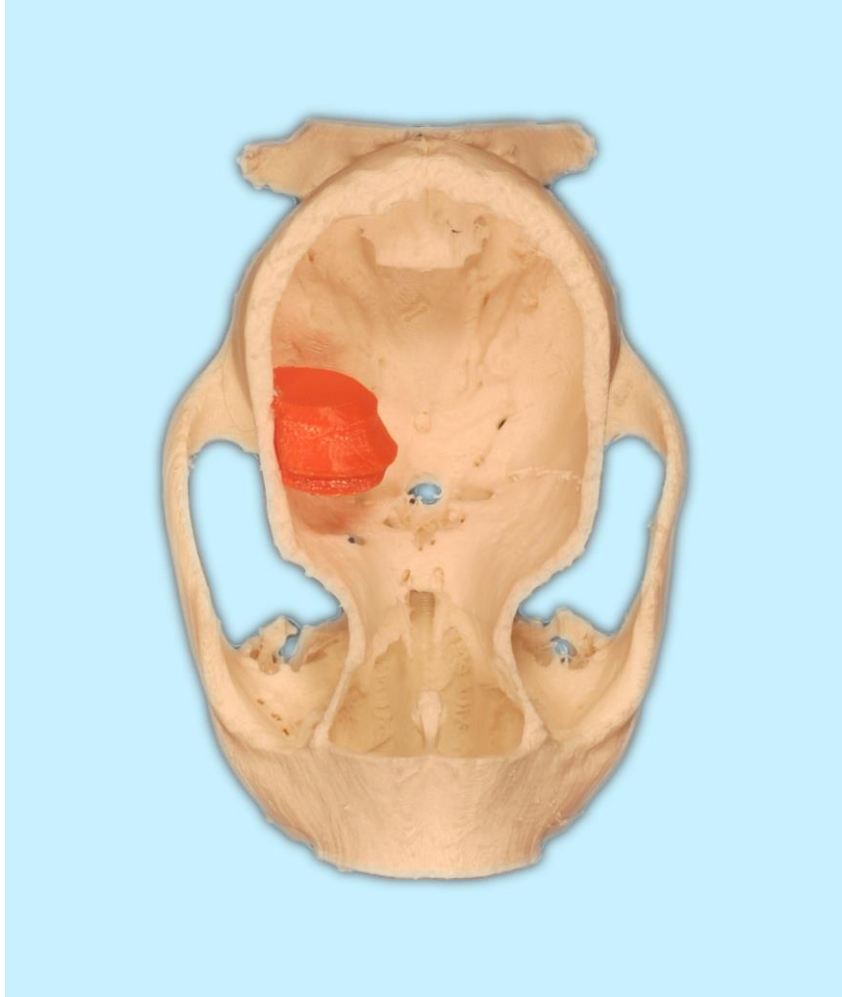
**b:** 3D STL model of the segmented structures.

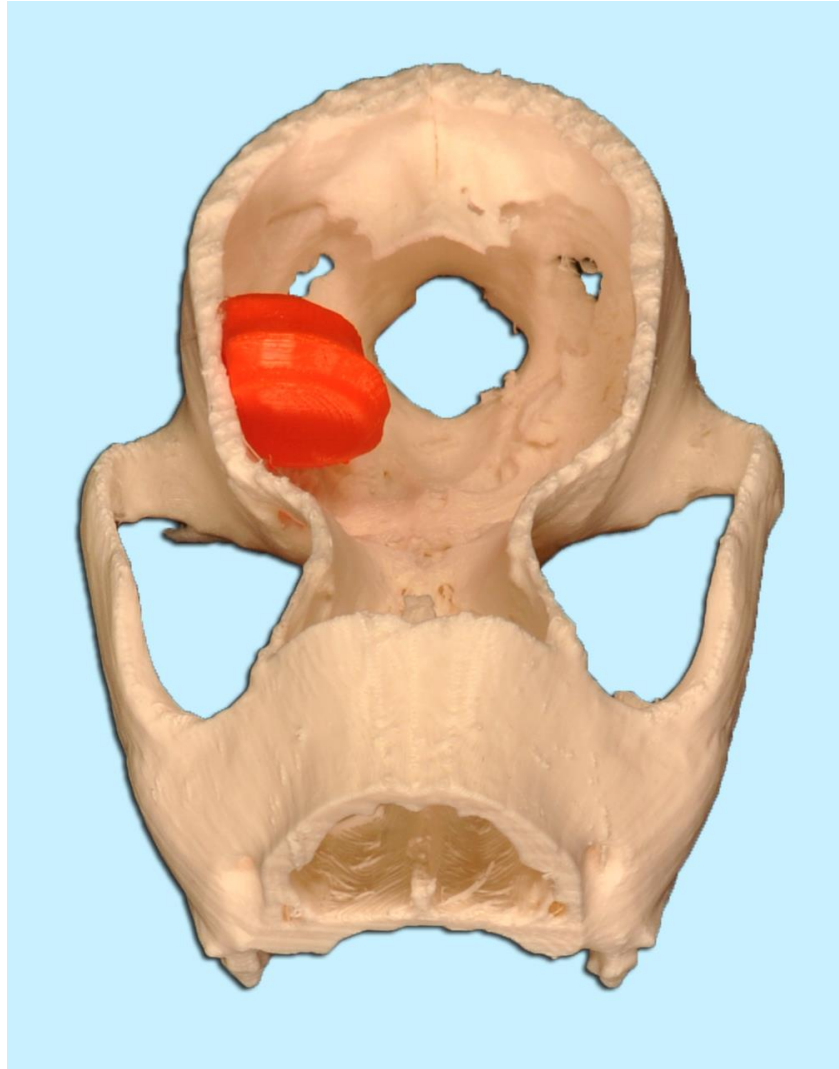
**c:** Rapid prototype created by the addition of material layers.



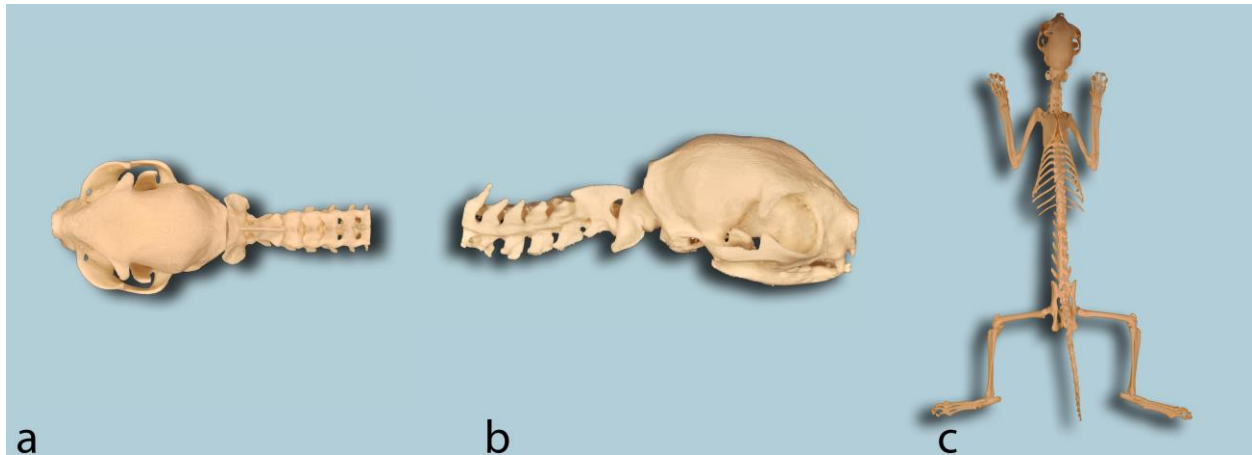
**Figure 2 (a, b and c):** Dorsoventral view (a) of a model of a cervical spine centered at the level of the atlanto-axial luxation. Note the two bent plates and surgical screws applied on the ventral aspect of the spine. These plates were used as a template to bend the actual surgical plates in surgery (model printed using transparent PLA on a Replicator2, Makerbot, Brooklyn, NY at 230 degrees celsius, and a resolution of 200 microns).  
Computer rendered illustrations of the same atlanto-axial luxation, dorsoventral (b) and right lateral projection (c).





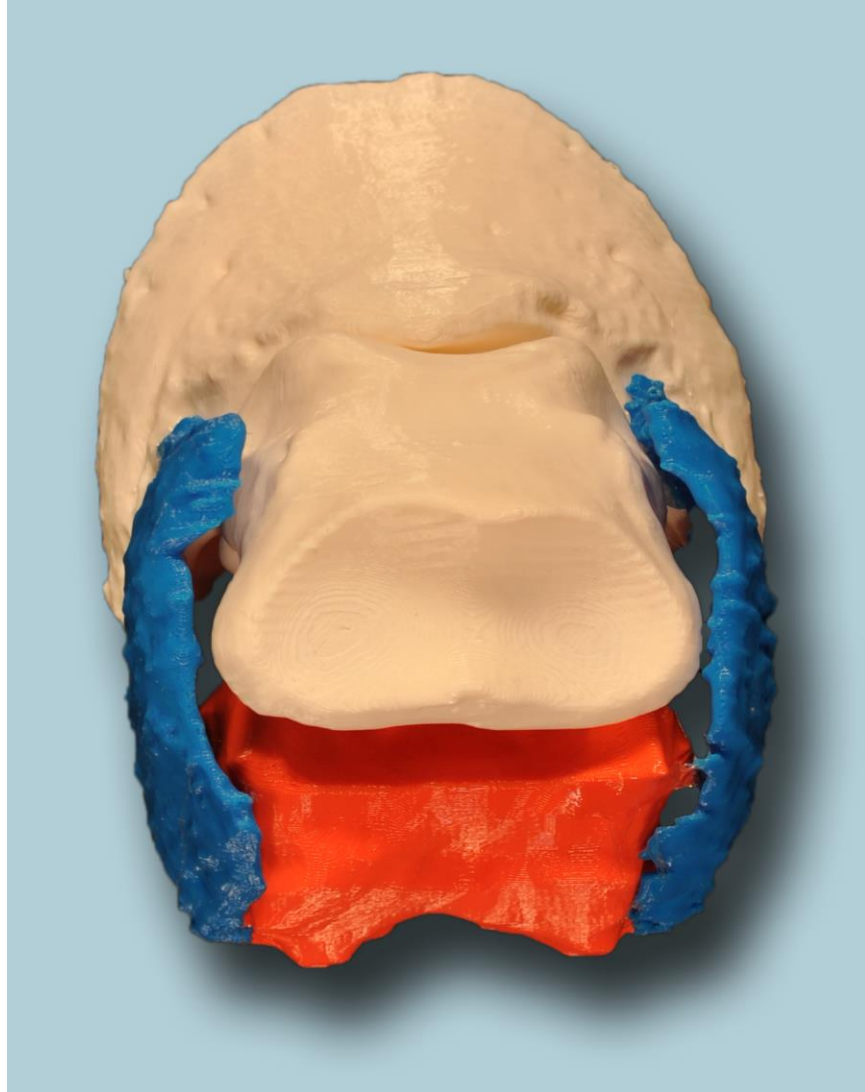


**Figure 3 (a and b):** Dorsoventral (a) and oblique (b) view of a model of an open cranium, in which a brain tumor has been reconstructed. The model was printed using a colored thermoplastic material on a Replicator2 3D printer (Makerbot, Brooklyn, NY) at 230 degrees celsius with a resolution of 200 microns.



**Figure 4 (a, b and c):**

**a, b and c:** (a) Ventrodorsal, (b) lateral view of a prototype based on healthy cat (from the skull to the level of C7), and (c): full skeleton of a non-affected cat, which will be used as a comparison with cats affected with GM2 Gangliosidosis. The model was printed using colored thermoplastic material on a Replicator2 3D printer (Makerbot, Brooklyn, NY) at 230 degrees celsius with a resolution of 200 microns.



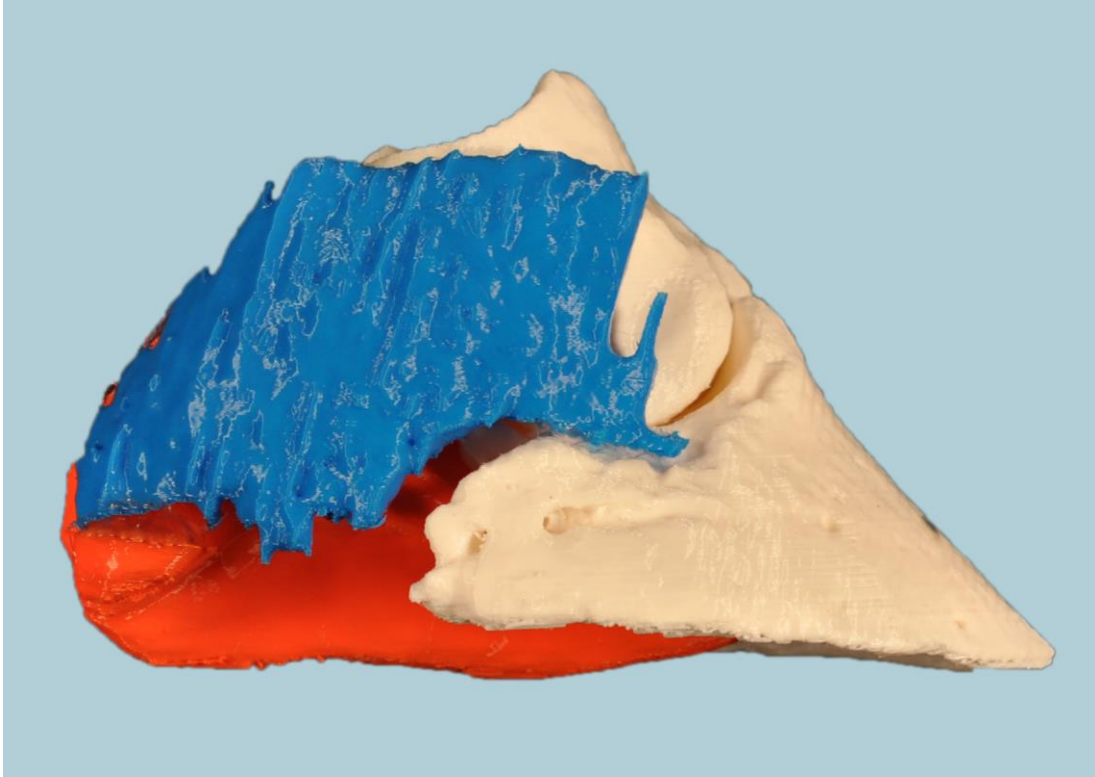


**Figure 5 (a and b):** Dorso-palmar (a) and lateral (b) views of a model of the distal extremity of a horse's feet. The second and third phalanges are represented in white, the accessory cartilages in blue, and the digital cushion in orange. The model was printed using colored thermoplastic material on a Replicator2 3D printer (Makerbot, Brooklyn, NY) at 230 degrees celsius with a resolution of 200 microns.

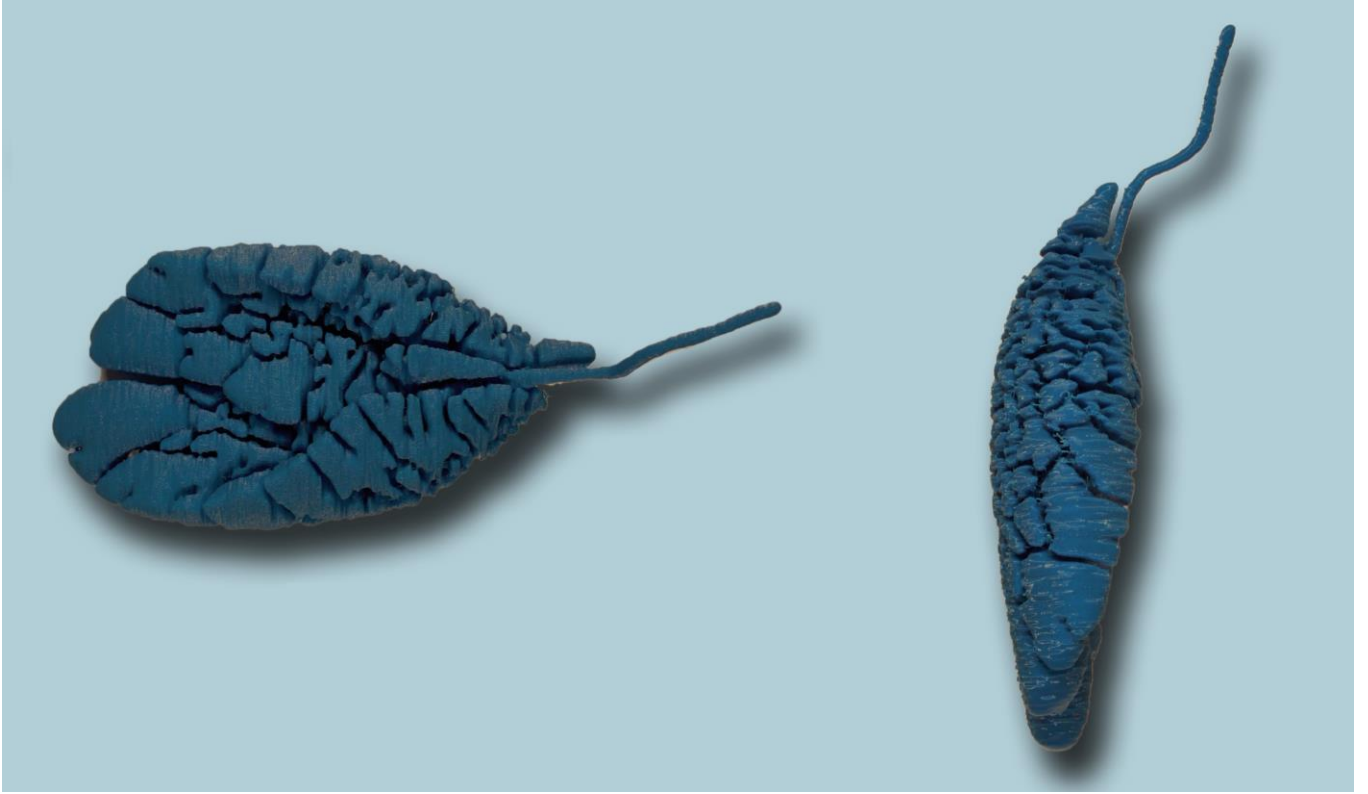




**Figure 6(a, b and c):** Dorsoventral (a) and lateral (b) views of a prototype of the bronchial tree of a Savannah Monitor lizard, (*Varanus exanthematicus* sp). (c) Dorsoventral view of a prototype of the bronchial tree of a Nile crocodile (*Crocodylus niloticus* sp). The model was printed using colored thermoplastic material on a Replicator2 3D printer (Makerbot, Brooklyn, NY) at 230 degrees celsius with a resolution of 200 microns.



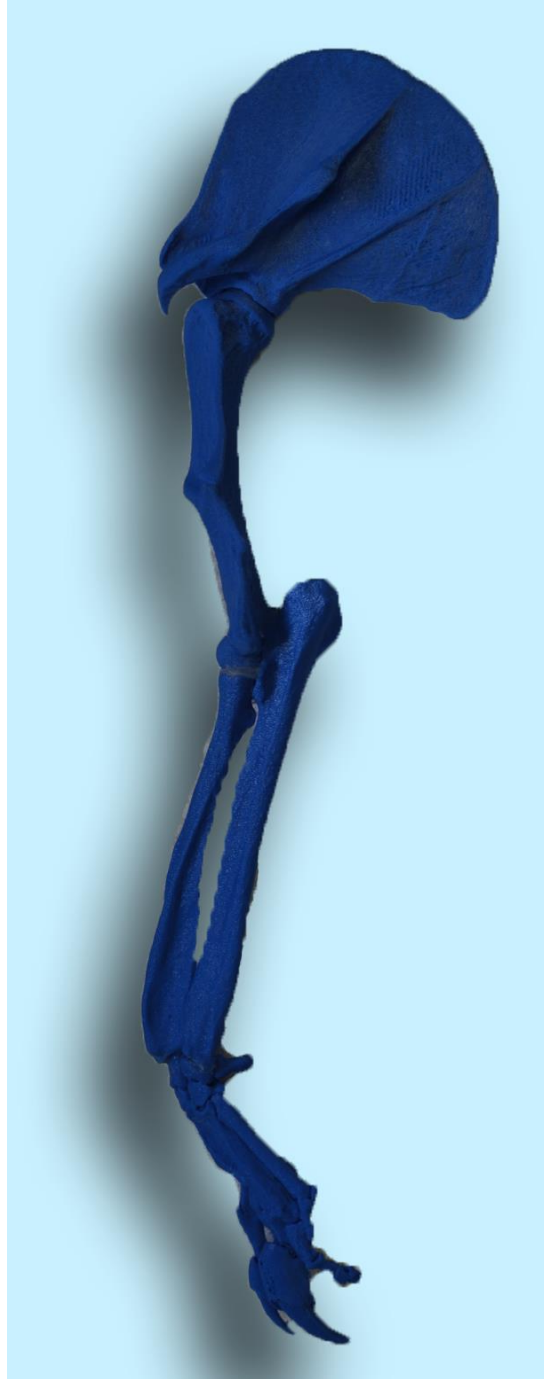


**Figure 7:** Lateral view of a model of the front limb of an Anteater (*Myrmecophaga Tridactyla*).

The model was printed using colored thermoplastic material on a Replicator2 3D printer (Makerbot, Brooklyn, NY) at 230 degrees celsius with a resolution of 200 microns.



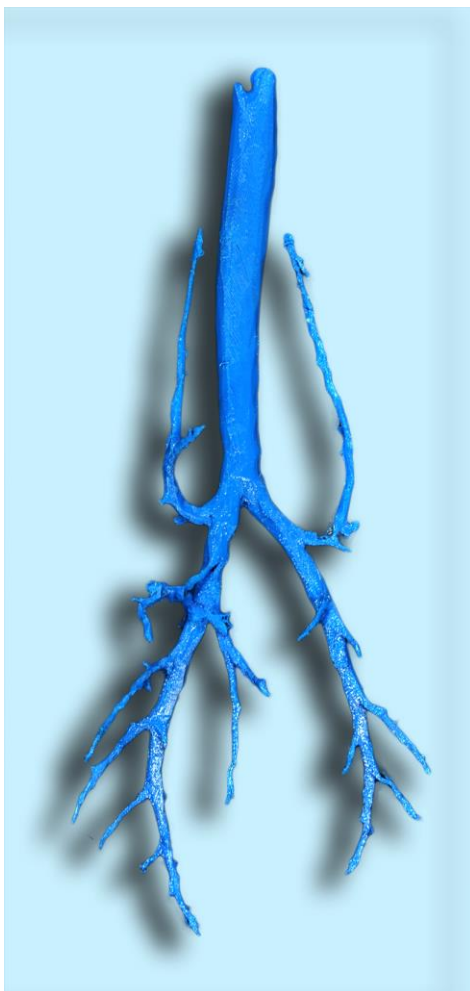


**Figure 8:** Dorsoventral view of a model of the bronchial tree of a healthy feline patient. This model was printed for use in the upper airway endoscopy room to illustrate landmarks and to serve as a teaching tool for students watching procedures. It was printed using colored thermoplastic material on a Replicator2 3D printer (Makerbot, Brooklyn, NY) at 230 degrees celsius with a resolution of 200 microns.

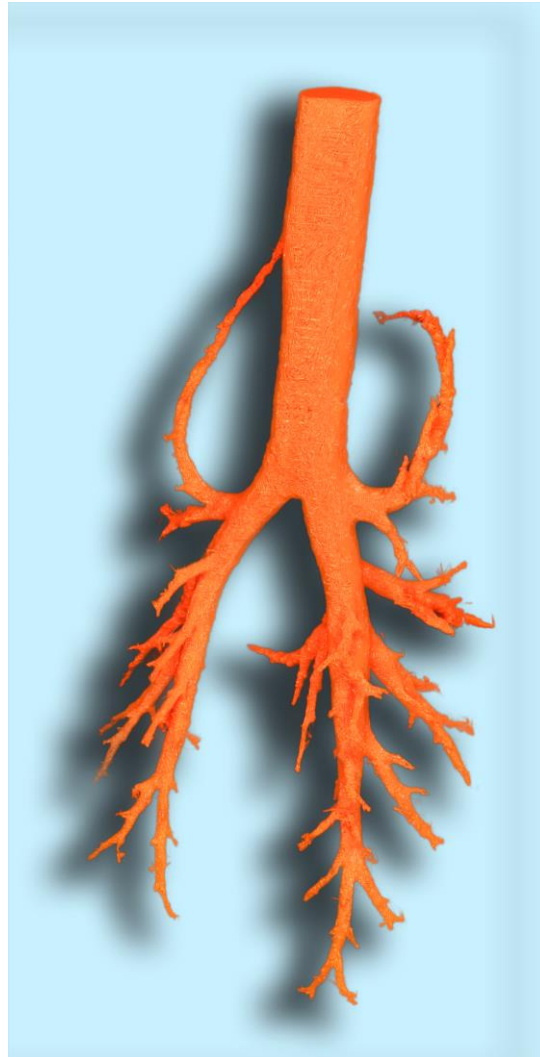


**Figure 9:** Dorsoventral view of a model of the bronchial tree of a healthy canine patient. This model was printed for use in the upper airway endoscopy room to illustrate landmarks and to serve as a teaching tool for students watching procedures. It was printed using colored thermoplastic material on a Replicator2 3D printer (Makerbot, Brooklyn, NY) at 230 degrees celsius with a resolution of 200 microns.



**Figure 10:** Lateral view of a model of the front limb of a horse. The model is proportionally reduced in size compared to the actual limb. It was printed using colored thermoplastic material on a Replicator2 3D printer (Makerbot, Brooklyn, NY) at 230 degrees celsius with a resolution of 200 microns. A 25 cent coin (24.6mm in diameter) was added to indicate the scale.



**Figure 11:** Canine and feline mannequins used for the experiment. Before the osseous implantation.





**Figure 12:** Canine mannequin illustrating the positioning of the osseous implant.





**Figure 13:** Canine mannequin with the osseous model implanted. The “bones” were implanted through a medial approach leaving no visible scar.





**Figure 14:** Feline mannequin illustrating the positioning of the osseous implant.



**Figure 15:** Feline mannequin with the osseous model implanted. The “bones” were implanted through a medial approach leaving no visible scar.



## **Appendix 2: Tables**

**Table 1:** Cost associated with the printing of various anatomical specimen using a standard FDM desktop printer, and a resolution of 200 microns. (Replicator 2, Makerbot, Brooklyn, New York).

Type of model	Weight of the model	Cost of the final model.
<b>Dog Skull (Labrador)</b>	42g	\$2.1
<b>Femur (Cat)</b>	10g	\$0.50
<b>Skull and cervical vertebrae up to C7 (Cat)</b>	39g	\$1.95
<b>Dog Pelvis (Labrador)</b>	100g	\$5

Questions						
I	II	III	IV	V	VI	VII
5	5	5	5	3	3	5
3	3	4	4	3	3	5
2	2	2	2	3	3	2
4	4	5	5	3	3	5
4	4	4	4	3	3	5
4	4	2	2	3	3	3
5	5	5	5	5	5	5
4	4	4	4	3	3	4
5	5	4	4	3	3	5
3	3	4	4	4	4	5
5	5	5	5	4	4	5
4	4	4	4	3	3	5
5	5	5	5	5	5	5
4	4	5	5	3	3	4
1	1	3	3	5	5	5
4	4	2	3	1	1	3
4	4	5	5	3	3	5
5	5	4	4	3	3	5
5	5	4	4	4	4	5
4	4	3	3	2	4	3

5	5	4	4	2	2	5
3	3	4	4	3	3	4
5	5	4	4	3	4	5
5	5	4	4	3	3	5
3	3	4	4	2	2	5
4	4	4	4	3	4	5
4	4	4	4	4	3	5
4	4	4	4	4	4	4
1	1	4	4	2	2	4
4	4	2	2	2	2	4
5	5	5	5	5	5	5

**Table 2:** Summary of the 31 responses to the quality survey. The seven questions have been answered on a scale from 1 to 5. A score of one expresses a complete disagreement with the questions, while a score a 5 expresses a complete agreement.

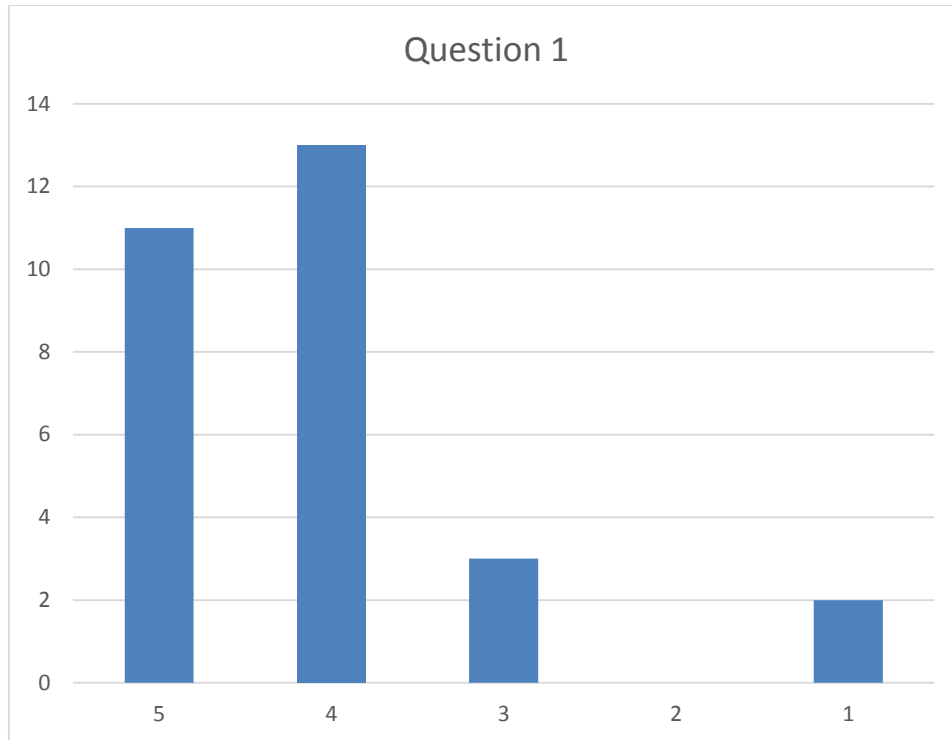


**Table 3:** Distribution of the responses to the first question (Scores on the X-axis, Number of responses on the Y-axes)

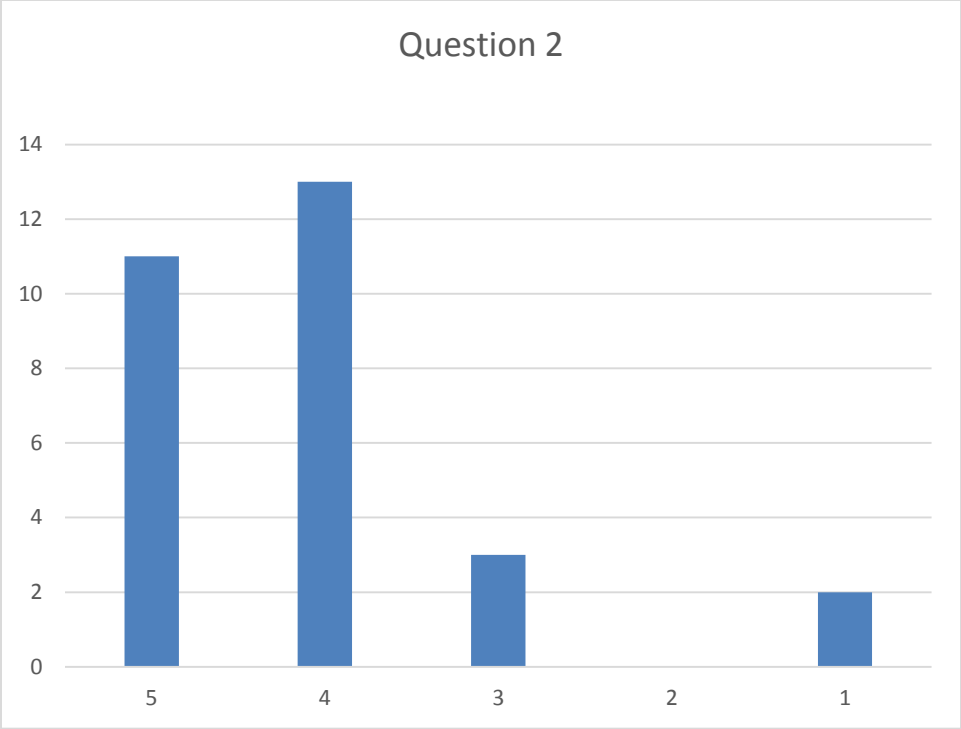


**Table 4:** Distribution of the responses to the second question (Scores on the X-axis, Number of responses on the Y-axes)

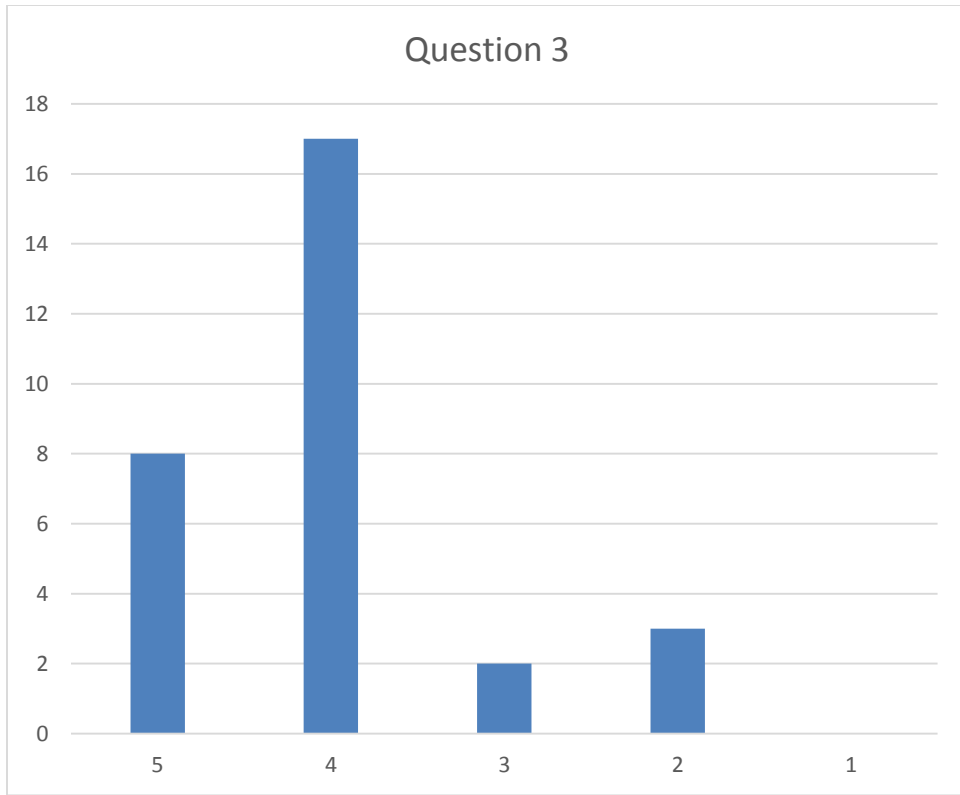


**Table 5:** Distribution of the responses to the third question (Scores on the X-axis, Number of responses on the Y-axes)

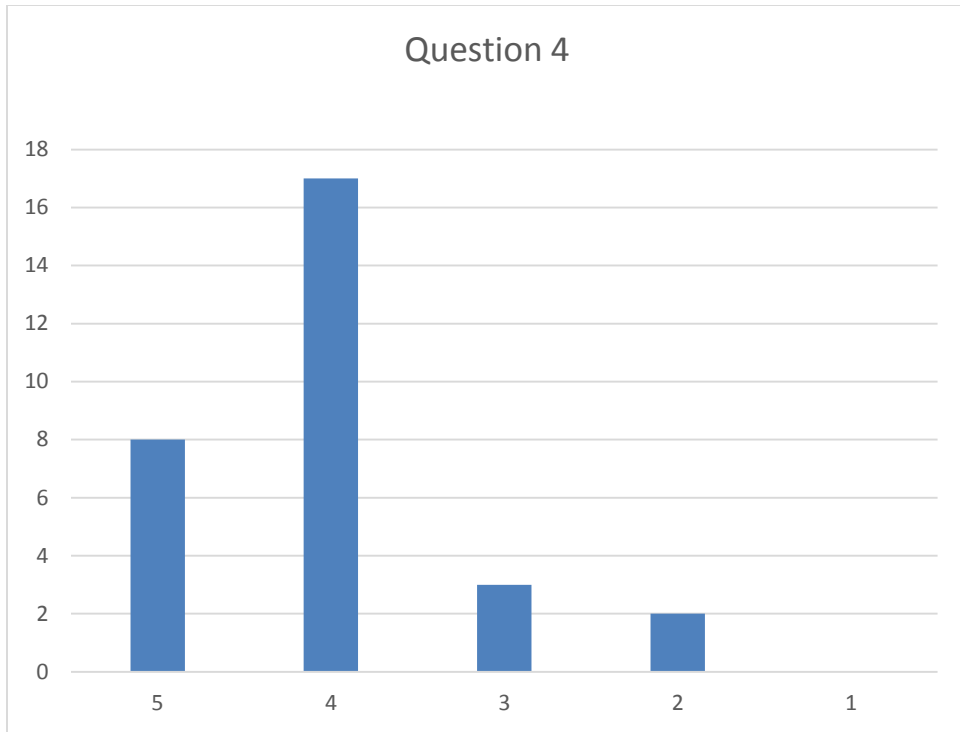


**Table 6:** Distribution of the responses to the fourth question (Scores on the X-axis, Number of responses on the Y-axes)



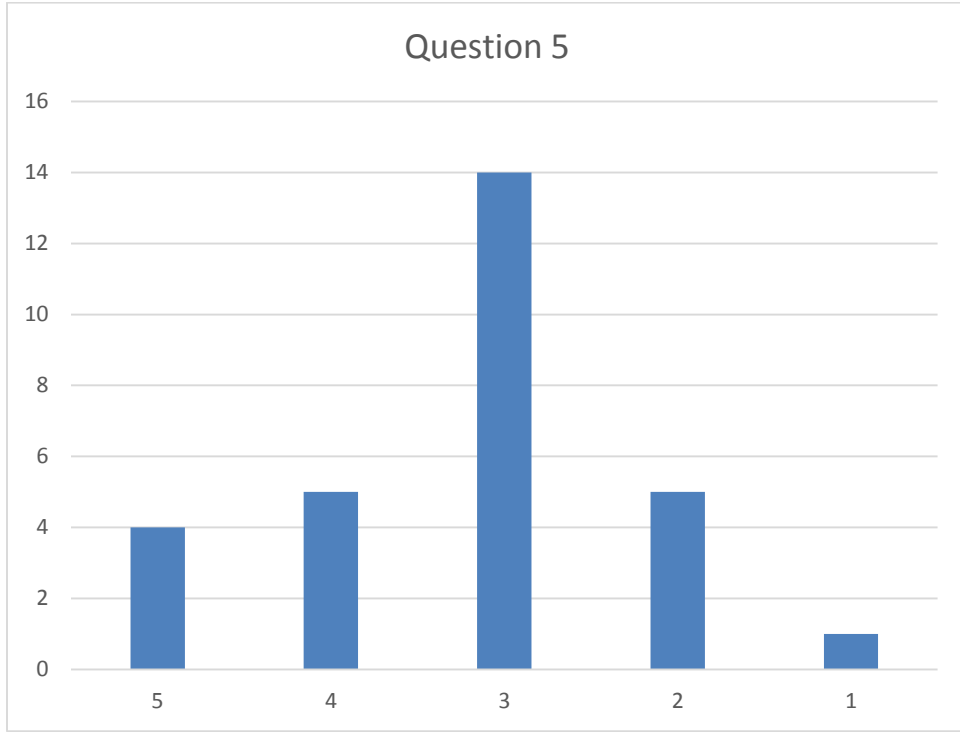


**Table 7:** Distribution of the responses to the fifth question (Scores on the X-axis, Number of responses on the Y-axes)

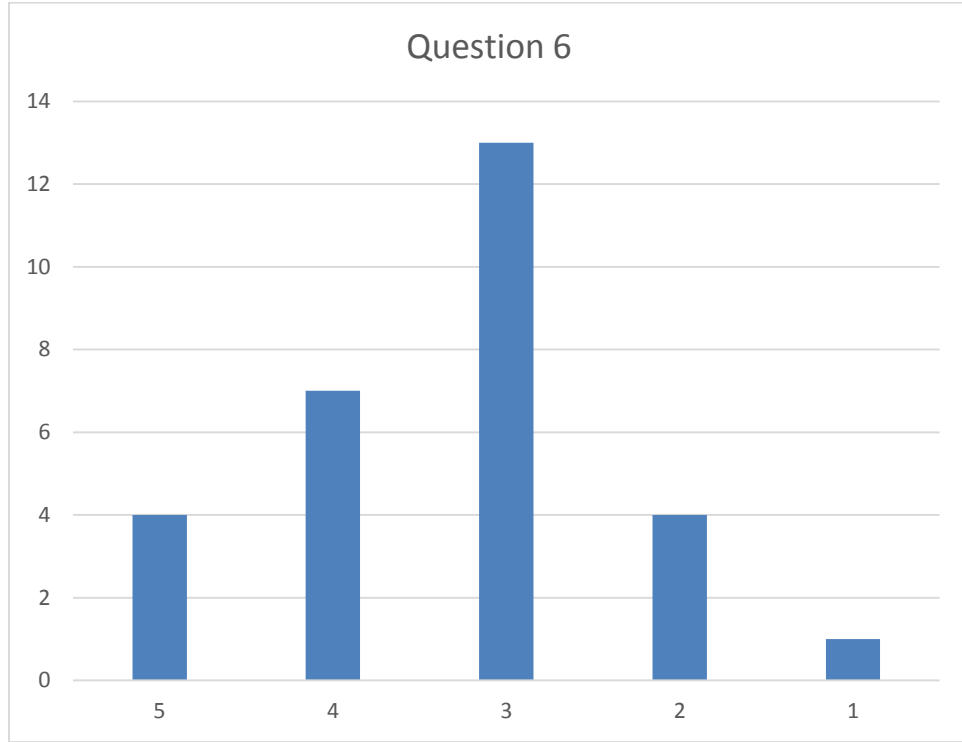


**Table 8:** Distribution of the responses to the sixth question (Scores on the X-axis, Number of responses on the Y-axes)

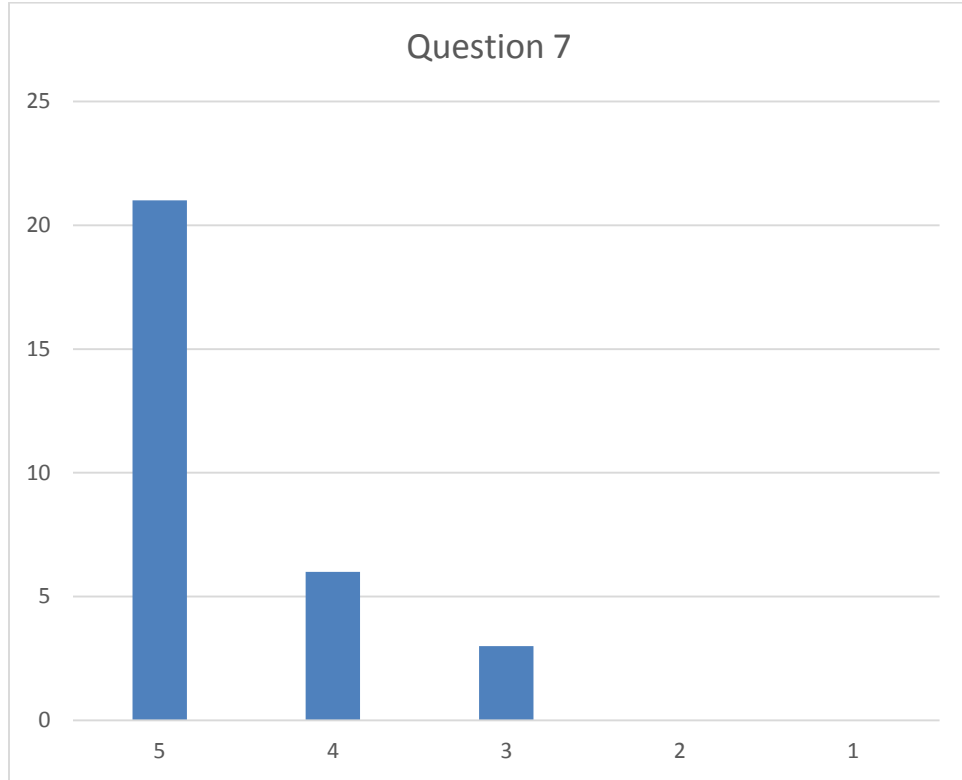


**Table 9:** Distribution of the responses to the seventh question (Scores on the X-axis, Number of responses on the Y-axes)

<b>N</b>	<b>Mean</b>	<b>Std Dev</b>	<b>Std Err</b>	<b>Minimum</b>	<b>Maximum</b>
123	4.2683	0.8305	0.0749	1.0000	5.0000

<b>Mean</b>	<b>95% CL Mean</b>	<b>Std Dev</b>	<b>95% CL Std Dev</b>
4.2683	4.1201 4.4165	0.8305	0.7381 0.9496

<b>DF</b>	<b>t Value</b>	<b>Pr &gt;  t </b>
122	16.94	<.0001

**Table 10:** Statistical parameters for the first question

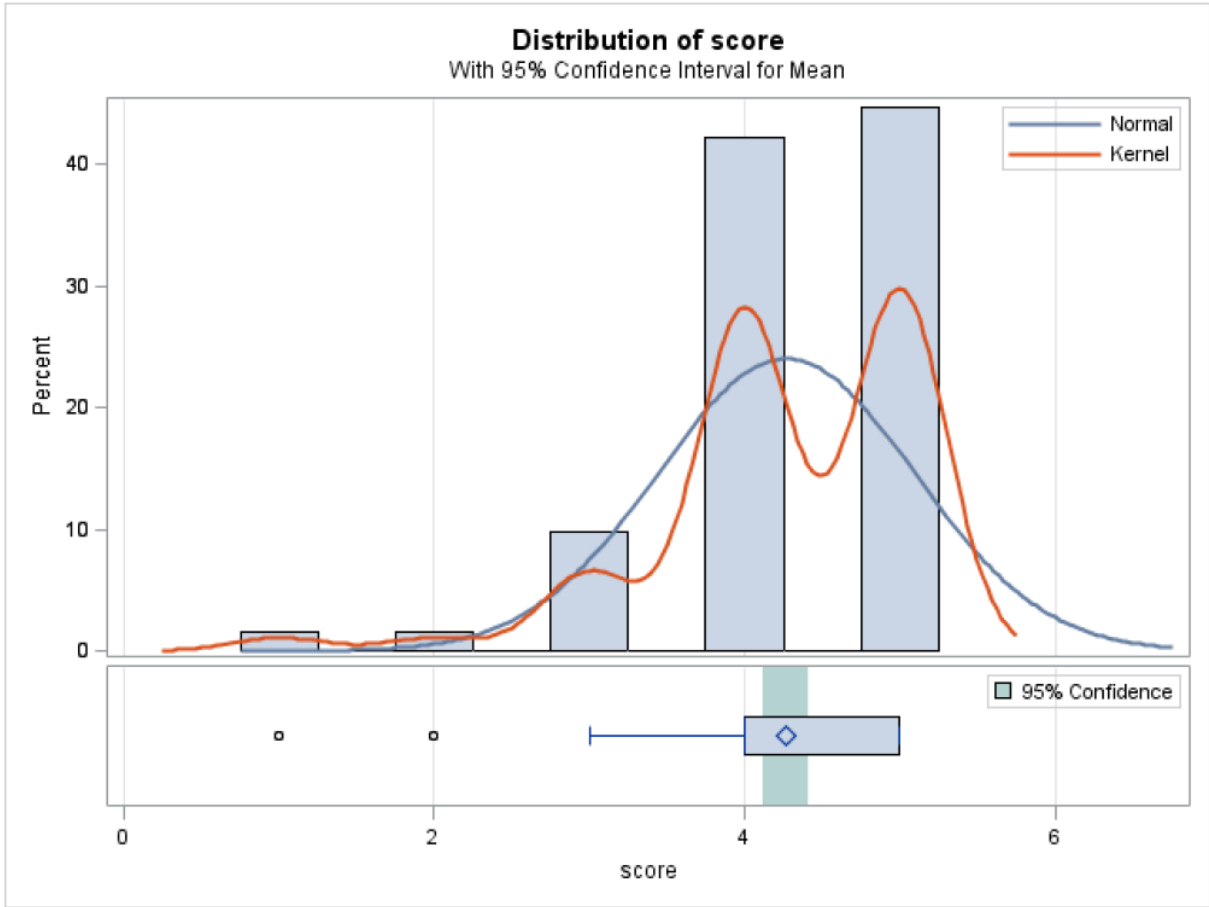


**Table 11:** Distribution of the responses to the first question

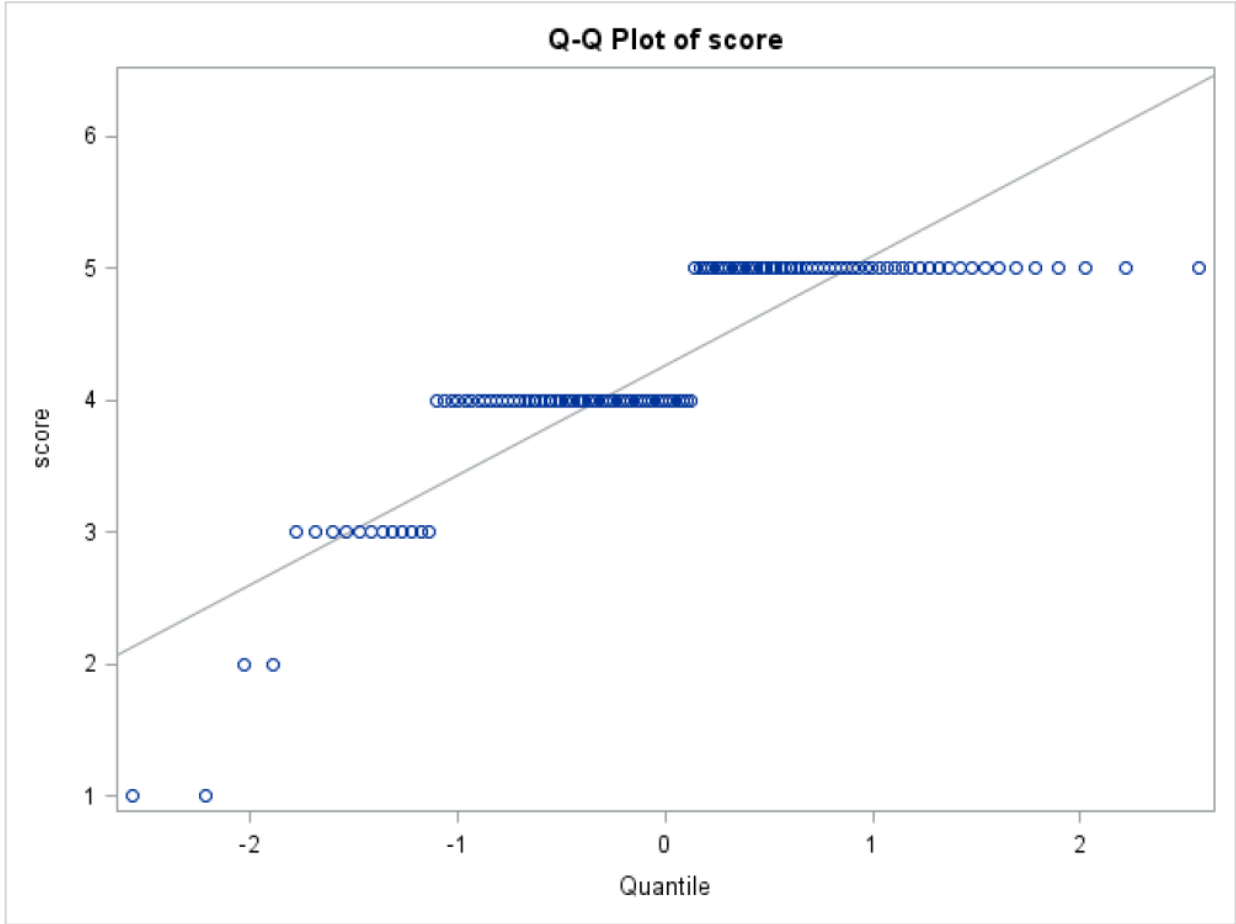


**Table 12:** Q-Q plot for the responses of the first question

<b>N</b>	<b>Mean</b>	<b>Std Dev</b>	<b>Std Err</b>	<b>Minimum</b>	<b>Maximum</b>
123	4.2683	0.8305	0.0749	1.0000	5.0000

<b>Mean</b>	<b>95% CL Mean</b>	<b>Std Dev</b>	<b>95% CL Std Dev</b>
4.2683	4.1201 4.4165	0.8305	0.7381 0.9496

<b>DF</b>	<b>t Value</b>	<b>Pr &gt;  t </b>
122	16.94	<.0001

**Table 13:** Statistical parameters for the second question

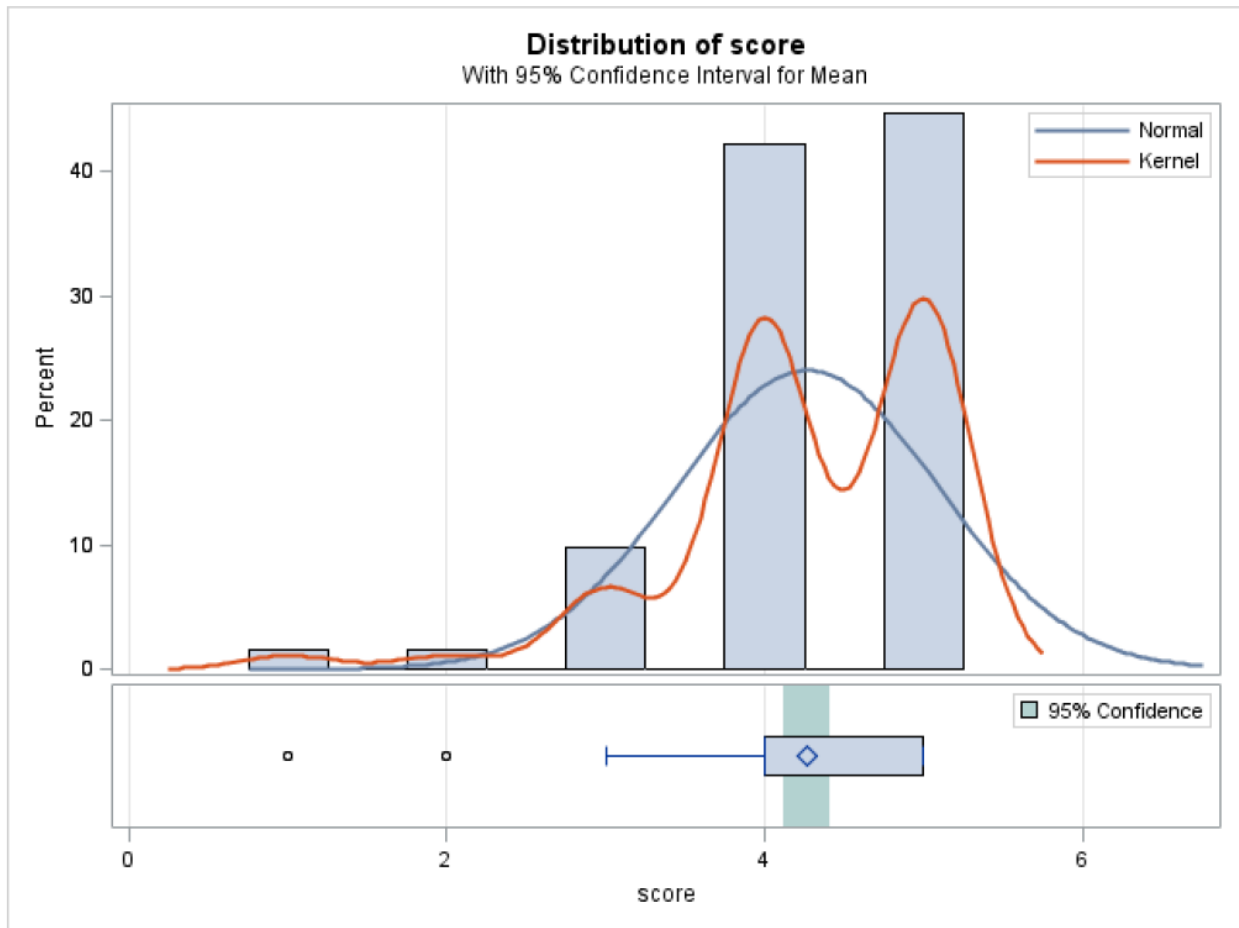


**Table 14:** Distribution of the responses to the second question



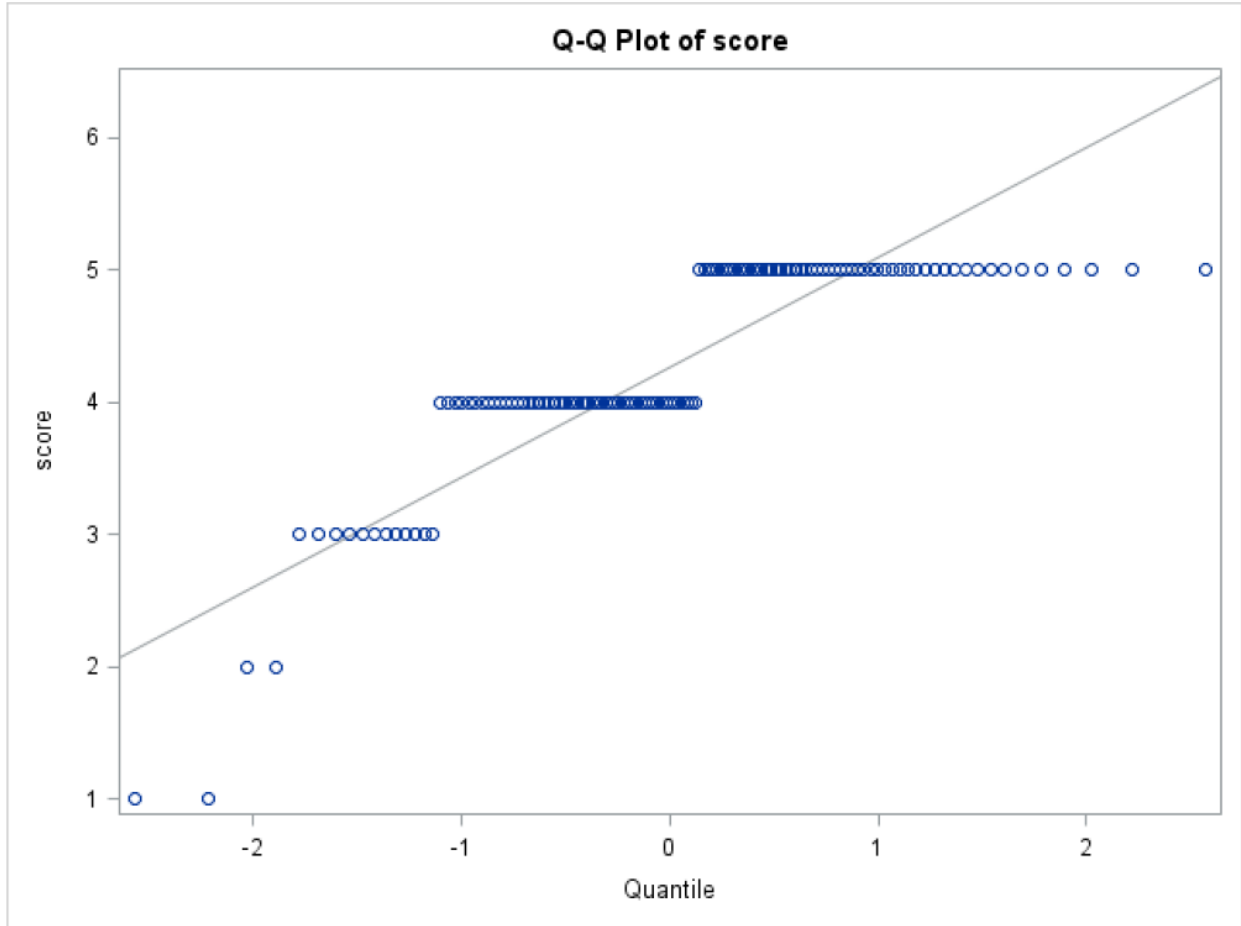


**Table 15:** Q-Q plot for the responses of the second question

<b>N</b>	<b>Mean</b>	<b>Std Dev</b>	<b>Std Err</b>	<b>Minimum</b>	<b>Maximum</b>
122	4.1475	0.7891	0.0714	2.0000	5.0000

<b>Mean</b>	<b>95% CL Mean</b>	<b>Std Dev</b>	<b>95% CL Std Dev</b>
4.1475	4.0061 4.2890	0.7891	0.7010 0.9028

<b>DF</b>	<b>t Value</b>	<b>Pr &gt;  t </b>
121	16.06	<.0001

**Table 16:** Statistical parameters for the third question

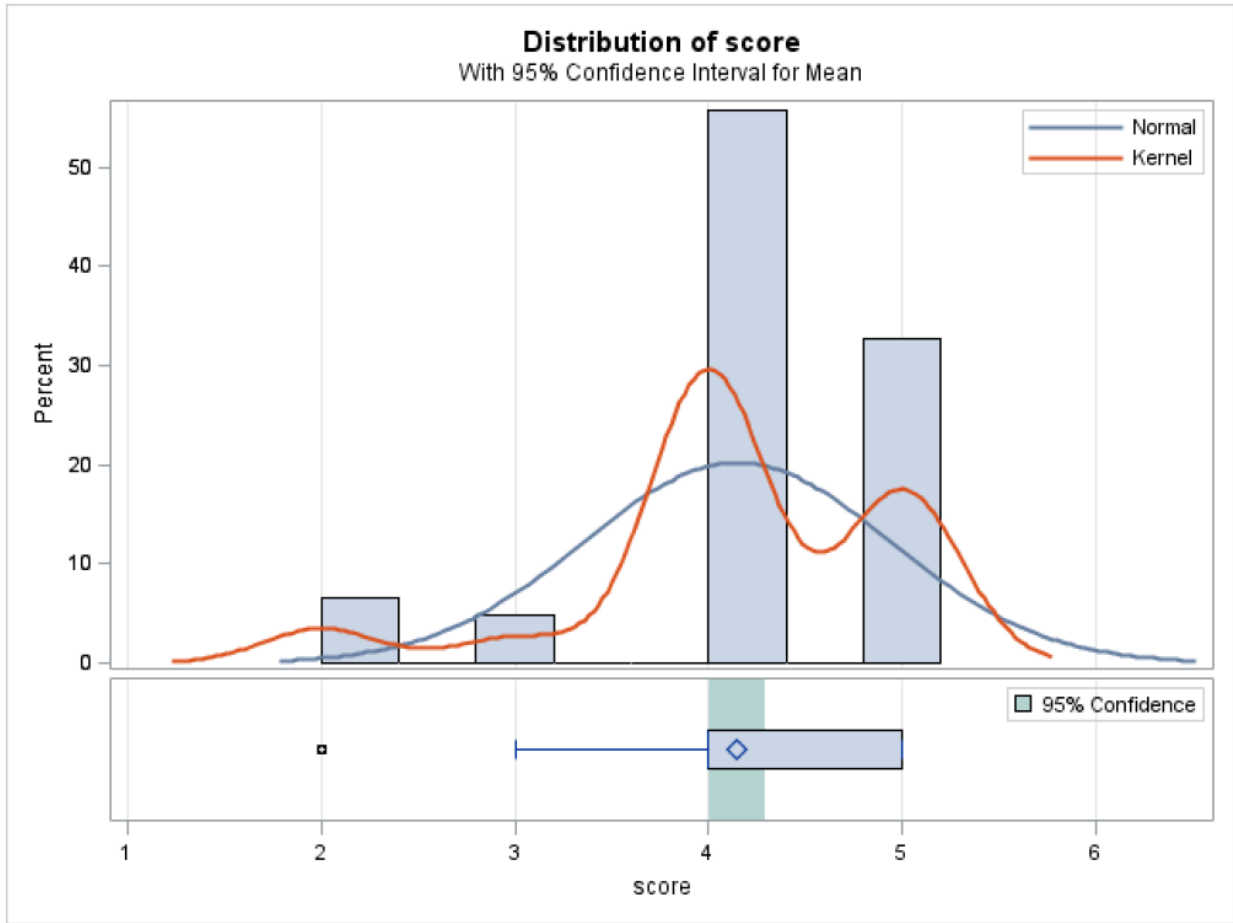


**Table 17:** Distribution of the responses to the third question

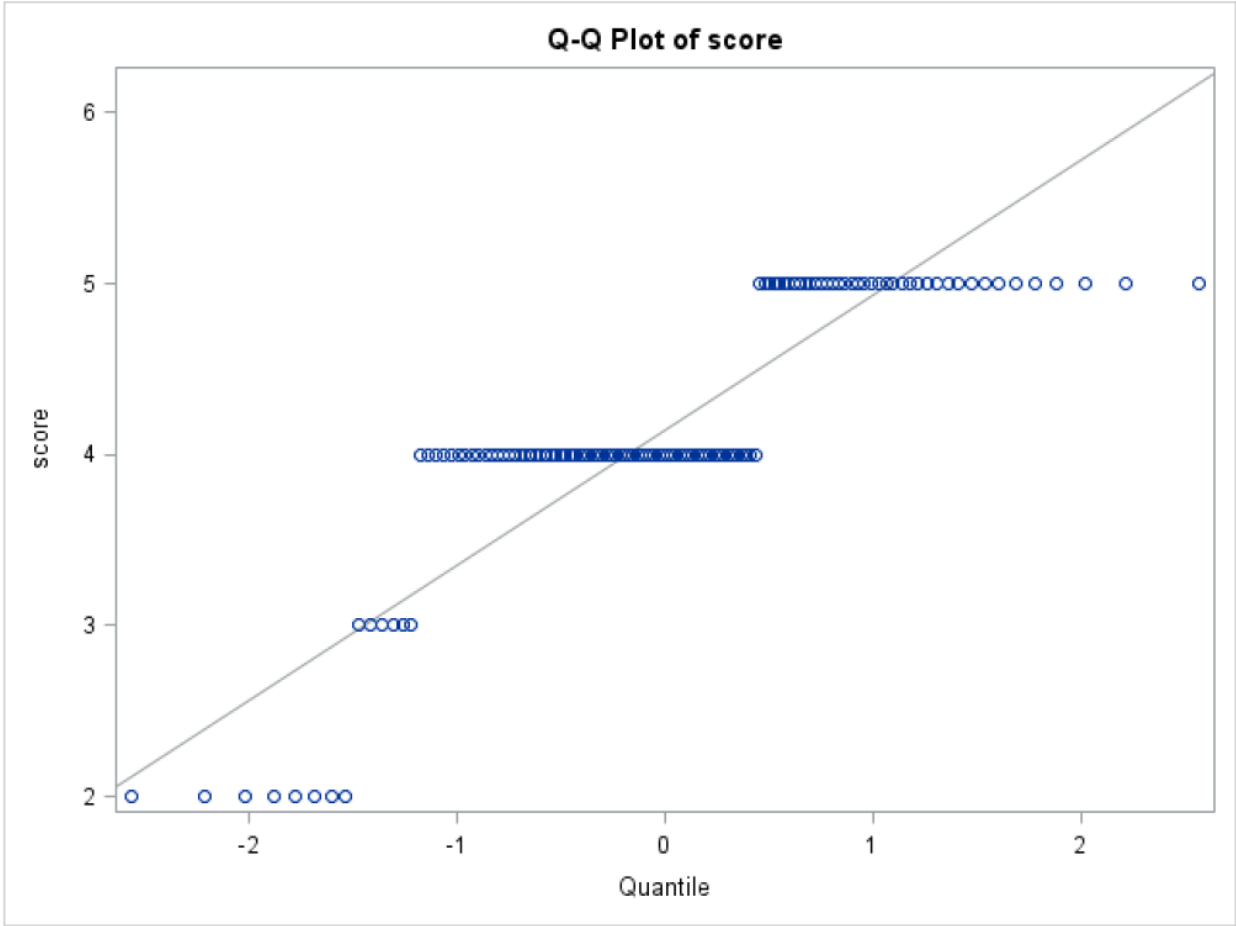


**Table 18:** Q-Q plot for the responses of the third question

<b>N</b>	<b>Mean</b>	<b>Std Dev</b>	<b>Std Err</b>	<b>Minimum</b>	<b>Maximum</b>
123	4.1545	0.7578	0.0683	2.0000	5.0000

<b>Mean</b>	<b>95% CL Mean</b>	<b>Std Dev</b>	<b>95% CL Std Dev</b>
4.1545	4.0192 4.2897	0.7578	0.6735 0.8665

<b>DF</b>	<b>t Value</b>	<b>Pr &gt;  t </b>
122	16.90	<.0001

**Table 19:** Statistical parameters for the fourth question

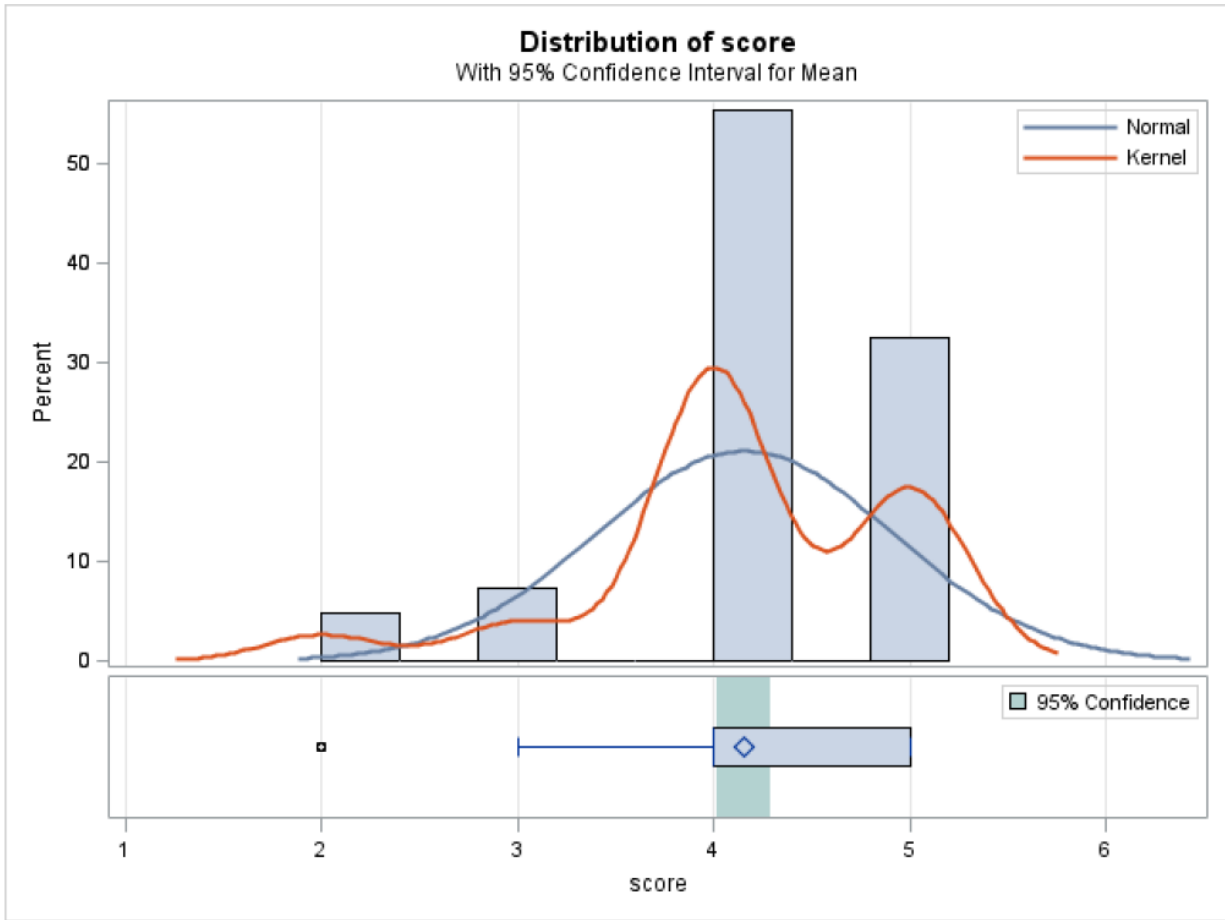


**Table 20:** Distribution of the responses to the fourth question

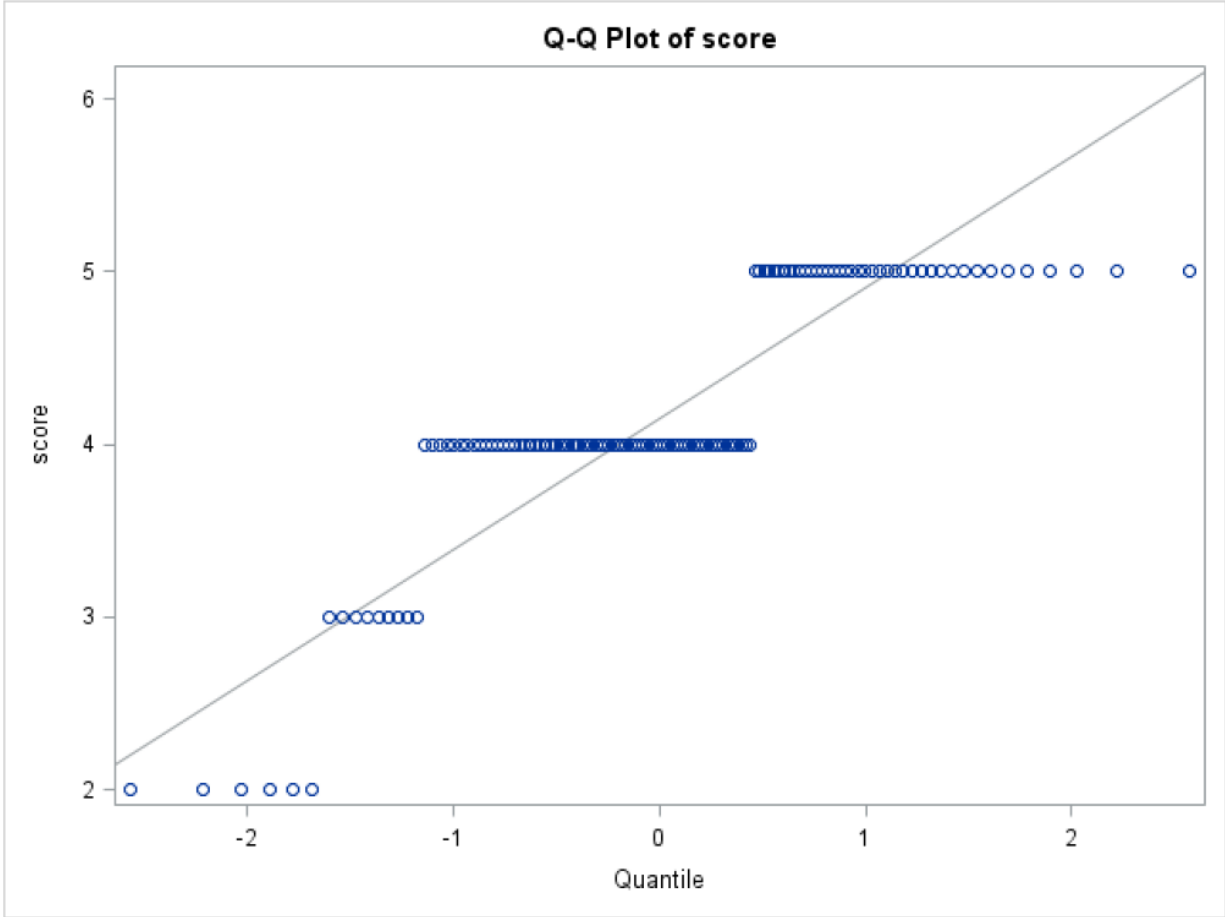


**Table 21:** Q-Q plot for the responses of the fourth question

<b>N</b>	<b>Mean</b>	<b>Std Dev</b>	<b>Std Err</b>	<b>Minimum</b>	<b>Maximum</b>
99	3.4848	0.9622	0.0967	1.0000	5.0000

<b>Mean</b>	<b>95% CL Mean</b>	<b>Std Dev</b>	<b>95% CL Std Dev</b>
3.4848	3.2929 3.6768	0.9622	0.8443 1.1187

<b>DF</b>	<b>t Value</b>	<b>Pr &gt;  t </b>
98	5.01	<.0001

**Table 22:** Statistical parameters for the fifth question



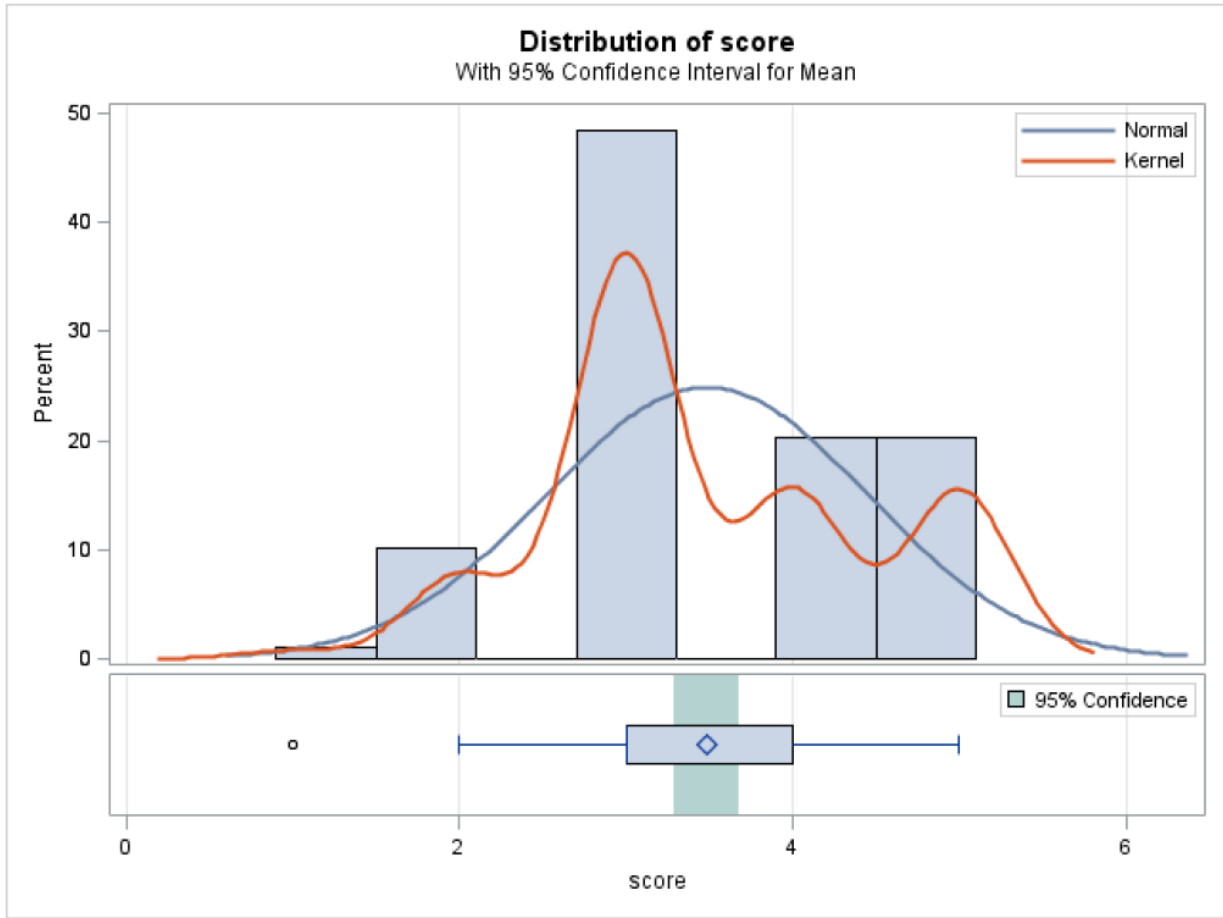


**Table 23:** Distribution of the responses to the fifth question

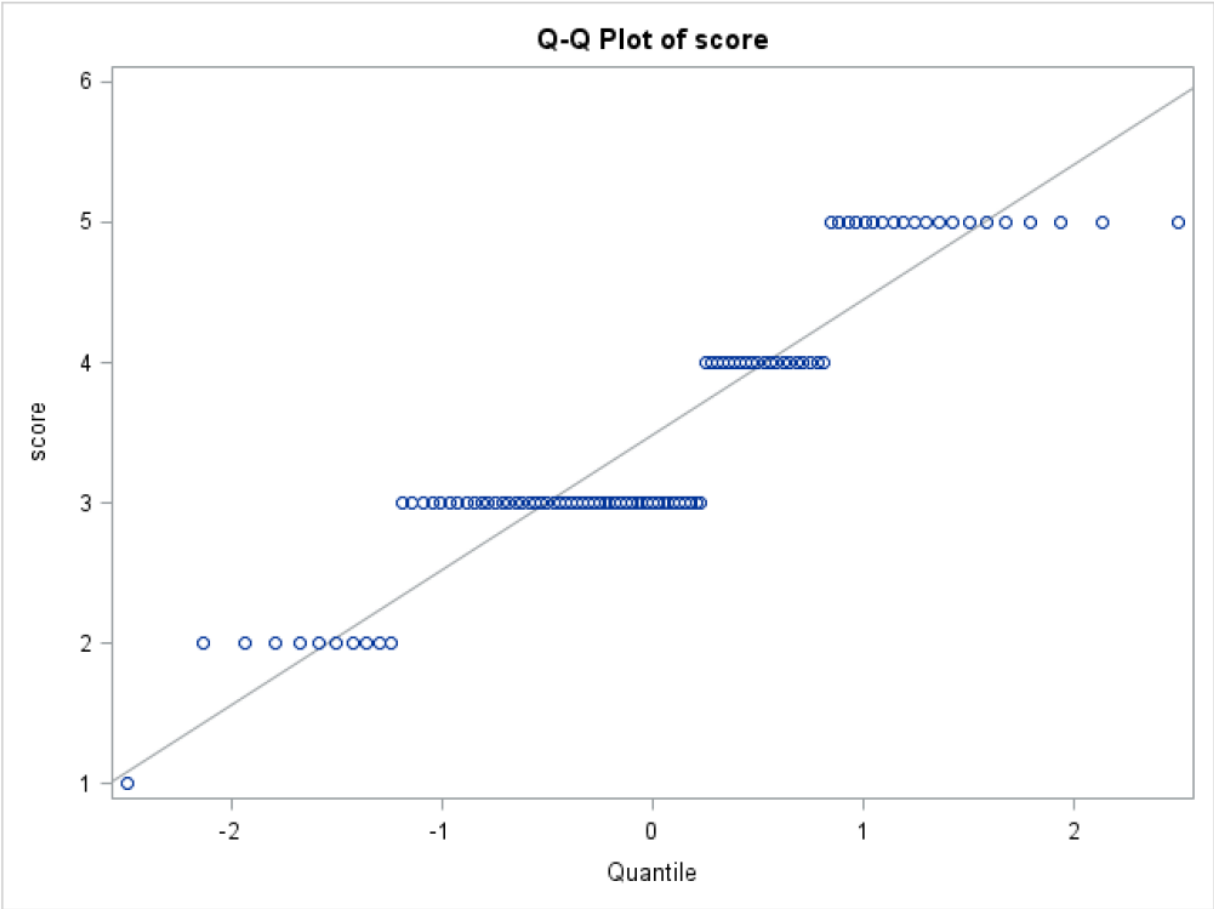


**Table 24:** Q-Q plot for the responses of the fifth question

<b>N</b>	<b>Mean</b>	<b>Std Dev</b>	<b>Std Err</b>	<b>Minimum</b>	<b>Maximum</b>
102	3.5686	0.9282	0.0919	1.0000	5.0000

<b>Mean</b>	<b>95% CL Mean</b>	<b>Std Dev</b>	<b>95% CL Std Dev</b>
3.5686	3.3863 3.7509	0.9282	0.8160 1.0766

<b>DF</b>	<b>t Value</b>	<b>Pr &gt;  t </b>
101	6.19	<.0001

**Table 25:** Statistical parameters for the sixth question

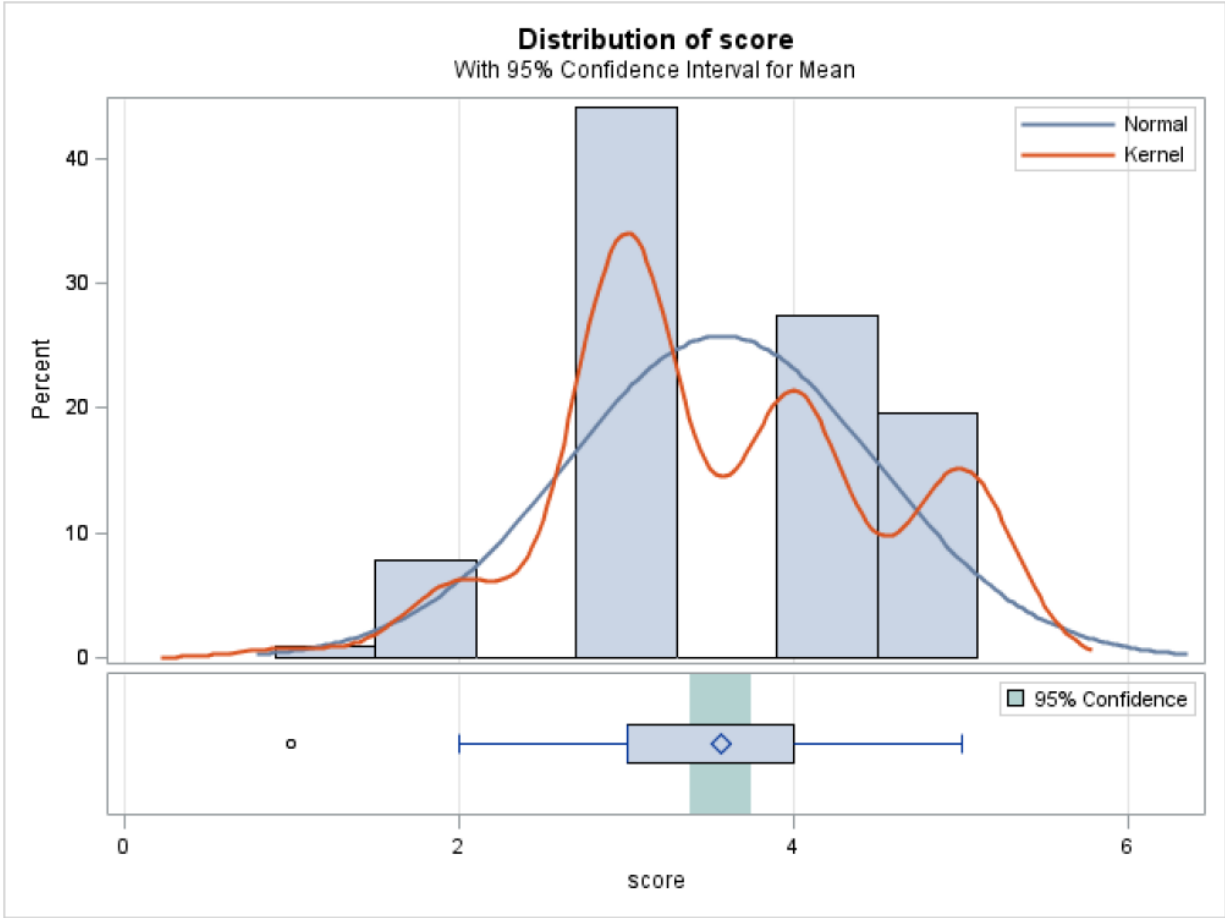


**Table 26:** Distribution of the responses to the sixth question

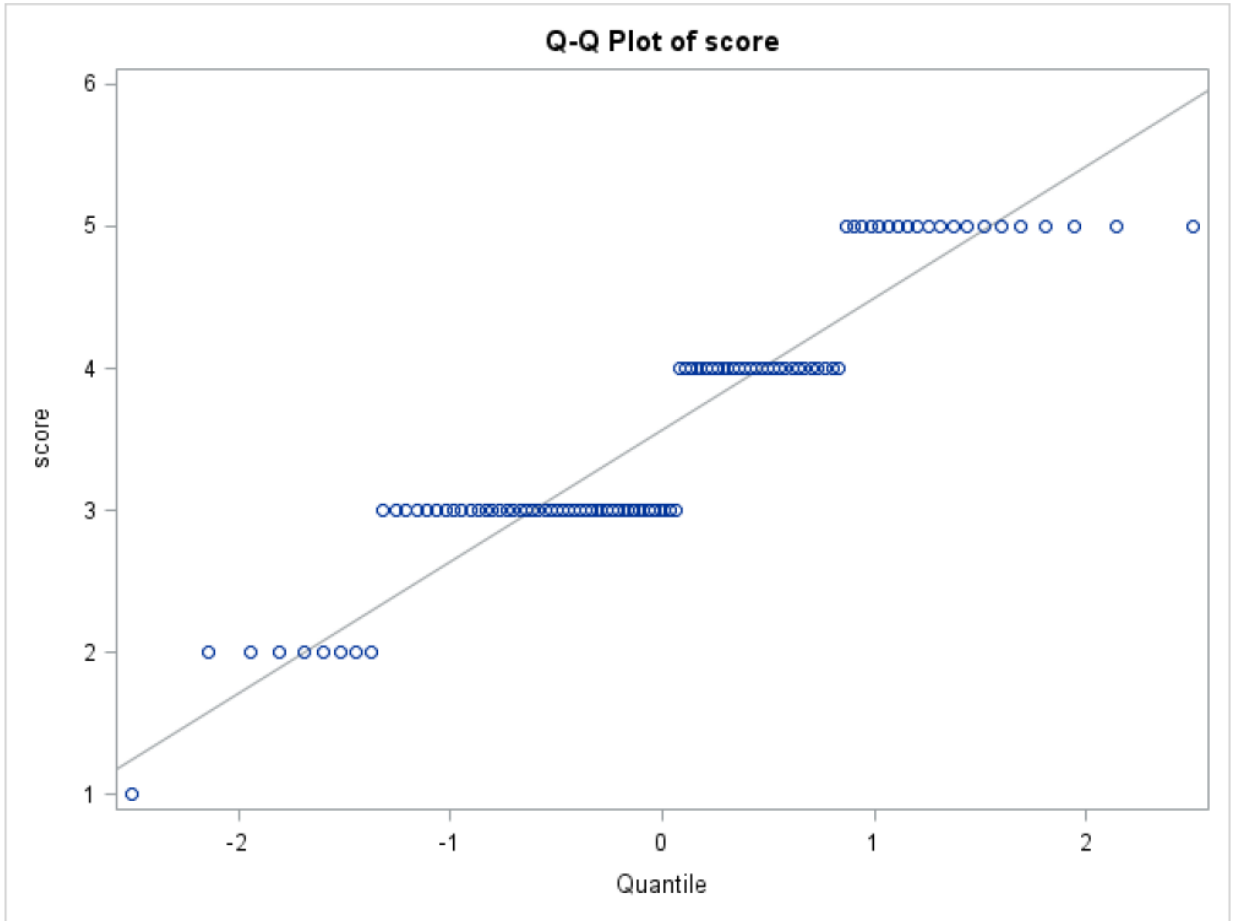


**Table 27:** Q-Q plot for the responses of the sixth question

<b>N</b>	<b>Mean</b>	<b>Std Dev</b>	<b>Std Err</b>	<b>Minimum</b>	<b>Maximum</b>
140	4.6571	0.6654	0.0562	2.0000	5.0000

<b>Mean</b>	<b>95% CL Mean</b>	<b>Std Dev</b>	<b>95% CL Std Dev</b>
4.6571	4.5460 4.7683	0.6654	0.5955 0.7540

<b>DF</b>	<b>t Value</b>	<b>Pr &gt;  t </b>
139	29.47	<.0001

**Table 28:** Statistical parameters for the seventh question

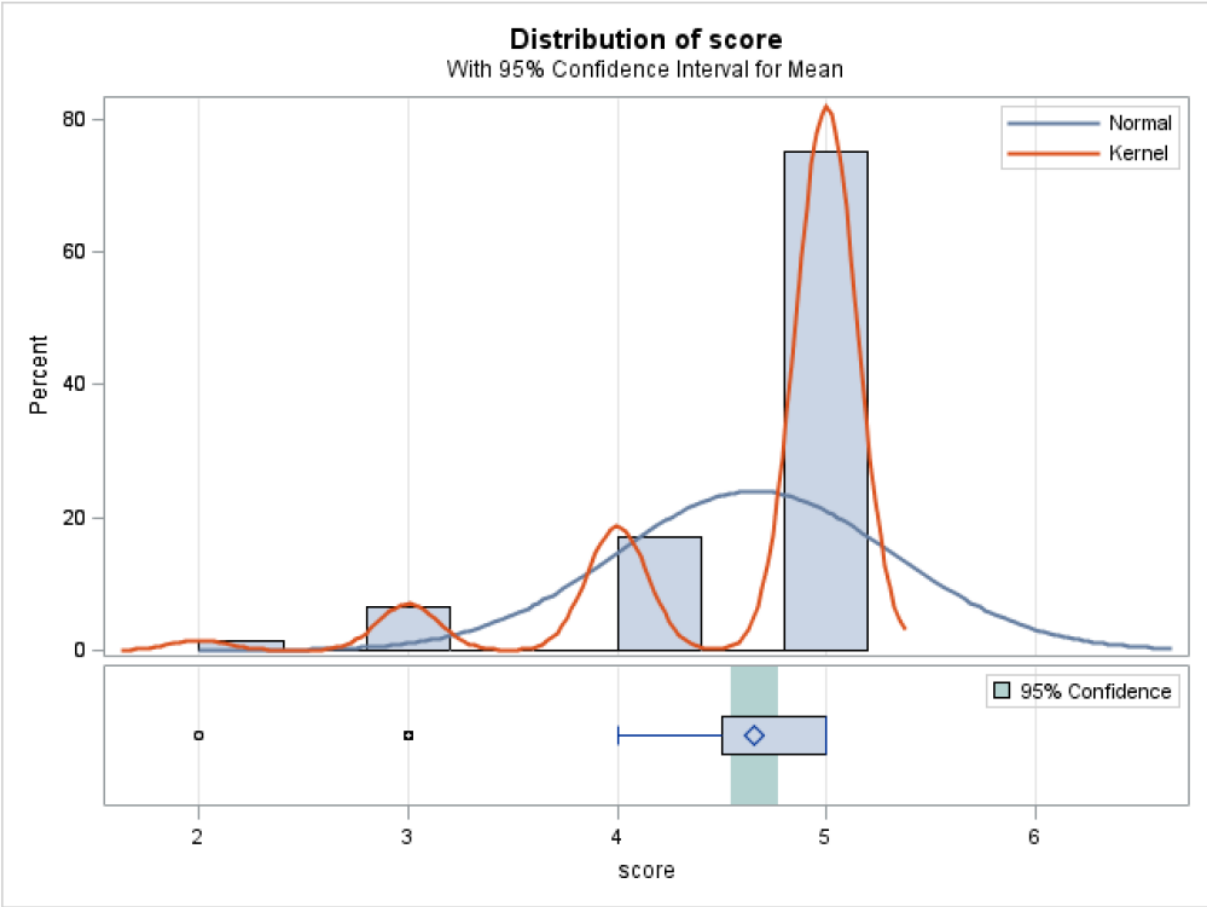


**Table 29:** Distribution of the responses to the seventh question

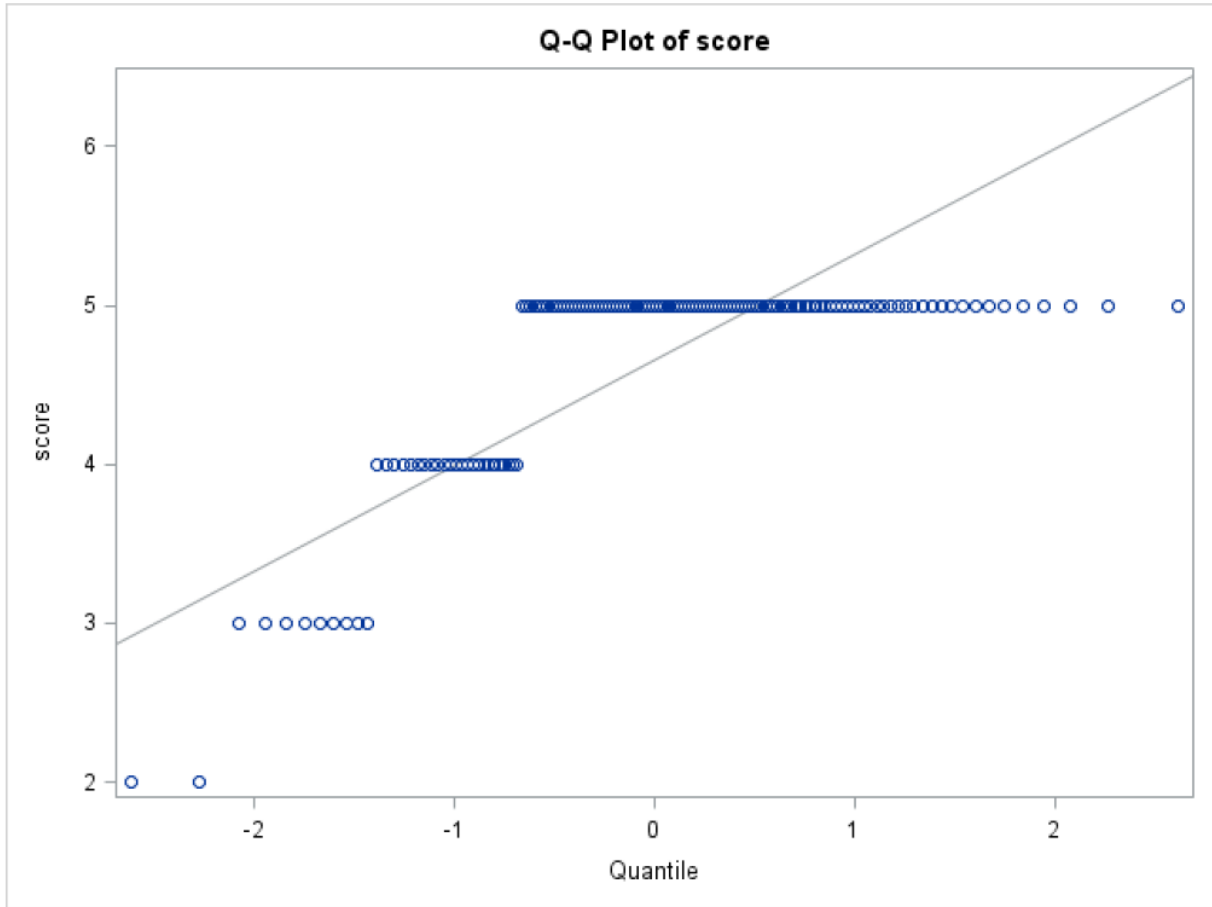


**Table 30:** Q-Q plot for the responses of the seventh question